REPORT NO. 73

THE BEHAVIOR OF TURBULENT BOUNDARY LAYERS IN ADVERSE PRESSURE GRADIENTS

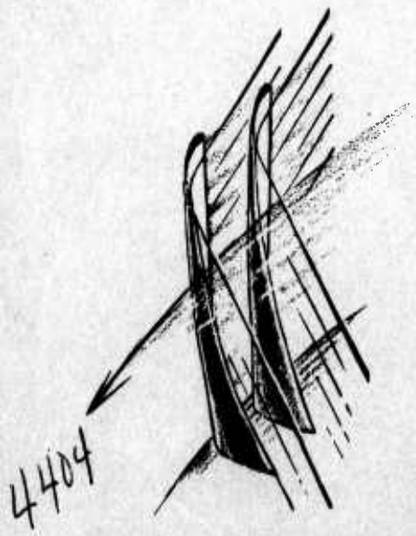

HAL L. MOSES

Research was carried out under the Bureau of Ships Fundamental Hydromechanics Research Program, S-R009 01 01, administered by the David Taylor Model Basin.

Contract Nonr 1841(91)

JANUARY 1964

GAS TURBINE LABORATORY
MASSACHUSETTS INSTITUTE OF TECHNOLOGY
CAMBRIDGE · 39 · MASSACHUSETTS

(5) 348 400 Gas Turbine Lab., Mass. Inst. of Tech., Cambridge.

(6) # THE BEHAVIOR OF TURBULENT BOUNDARY LAYERS IN ADVERSE PRESSURE GRADIENTS

(10) by

HAL L. MOSES

Research was carried out under the Bureau of Ships Fundamental Hydromechanics Research Program, S-R009 01 01, administered by the David Taylor Model Basin.
(16) Proj. (15) Contract Nonr 1841(91)

GAS TURBINE LABORATORY
(14) REPORT No. 73

January 1964

MASSACHUSETTS INSTITUTE OF TECHNOLOGY
Cambridge, Massachusetts

4404

ABSTRACT

The problem of predicting the behavior of the incompressible turbulent boundary layer in an adverse pressure gradient is re-examined. An outline of the problem is given along with a brief summary of the work that has already been done, including both experimental correlations and approximate theories. The results of an experimental investigation are presented for a separating turbulent boundary layer with various pressure distributions. An approximate theory is developed in which the momentum integral equation is satisfied for each half of the boundary layer. The velocity profiles used in the analysis consist of the well known wall and wake regions, resulting in a two-parameter family with the Reynolds number as one parameter. It is assumed, with some experimental justification, that the eddy viscosity can be reasonably approximated from zero pressure gradient experiments. The numerical calculations, using the Runge-Kutta procedure, show good agreement with the experiments. ~~Finally,~~ the reliability that can be expected of such approximate methods is discussed, and the uncertainty ~~due to the turbulent shear stress~~ is examined for several general cases.

ACKNOWLEDGEMENTS

The author acknowleges, with gratitude, the advice and encouragement of his thesis committee: Professor Philip G. Hill, thesis supervisor, whose very helpful advice included the experimental apparatus; Professor Edward S. Taylor, Director of the Gas Turbine Laboratory; Professor Erik Mollo-Christensen of the Aeronautical and Astronautical Department; and Professor Howard Emmons of the Department of Mechanical Engineering at Harvard University.

He is also indebted to Mr. Stephen Portnoy for assisting with the computer work, Mr. John Macrae for the computations and curves and Mrs. Rose Tedmon, who helped with the typing.

Finally, the author would like to express his appreciation to the entire staff of the Gas Turbine Laboratory for their assistance in carrying out this work. He is especially grateful to Mr. I-Man Moon for helping with the hot-wire equipment, Mr. Brian Launder for reading the preliminary draft, Mr. Dalton Baugh and staff for constructing the apparatus and Mrs. Madelyn Euvrard for her assistance as typist, secretary and chairman of the coffee breaks.

The numerical calculations were done with the assistance of the M. I. T. Computation Center.

TABLE of CONTENTS

LIST of FIGURES

NOMENCLATURE

c_f Skin friction coefficient, $\tau_w / \frac{1}{2} \rho U^2$

C_p Pressure coefficient, $1 - (\frac{U}{U_1})^2$

H Shape factor (equation 9)

log Natural logarithm

P Static pressure

R_θ Reynolds number based on θ , $U\theta/\gamma$

R_δ Reynolds number based on δ , $U\delta/\gamma$

r Radius

T Time

U Free stream velocity

u_τ Friction velocity, $\sqrt{\tau_w/\rho}$

u Component of velocity parallel to the wall (time average)

u' Component of velocity parallel to the wall (fluctuating)

v Component of velocity normal to the wall (time average)

v' Component of velocity normal to the wall (fluctuating)

w Wake function (equations 49 and 50)

x Distance along the wall (flow direction)

y Distance normal to the wall

z Distance normal to x and y

α Boundary layer parameter (equations 57 and 58)

β Boundary layer parameter (equations 58 and 59)

Γ Form parameter (equation 19)

δ Boundary layer thickness

δ^* Displacement thickness (equation 8)

δ^{**} Energy Thickness (equation 14)

ϵ Eddy viscosity (equation 30)

η y/δ

θ Momentum thickness (equation 7)

λ Ratio of pressure to shear forces (equation 44)

ν Kinematic viscosity

Π Wake parameter (equation 49)

ρ Density

τ Shear stress

τ_w Shear stress at the wall

ω Angle of three-dimensional flow (equation 38)

I. INTRODUCTION

The behavior of the turbulent boundary layer in an adverse pressure gradient is probably one of the most important and also one of the most difficult problems in fluid mechanics. Almost all devices involving fluid flow, such as pumps, compressors, diffusers, airfoils and submerged bodies, depend critically upon this behavior. The effort that has been expended on this one problem gives evidence of the difficulty as well as the importance.

The boundary layer concept was introduced in 1904 by L. Prandtl, who demonstrated that in many cases fluid flow could be divided into an essentially inviscid region and a thin viscous region near a solid surface. Although there are some exceptions, the inviscid flow theory is fairly complete. Because the viscous layer is relatively thin, the equations of motion can be simplified considerably in this region. However, much of the boundary layer theory that has been developed is for laminar flow, where a mathematical approach is at least possible, but in most applications the flow is turbulent.

In an adverse pressure gradient the fluid very near the solid surface that has been retarded by viscous forces quickly loses its remaining momentum. When this happens the boundary layer is likely to separate, or stall, and completely change the flow. The loss of momentum by the fluid near the wall, then, is the significant factor in the behavior of the boundary layer. Because of the mixing motion, the rate of transfer of momentum to the inner layers is much greater in turbulent flow, and separation is usually delayed relative to the laminar case.

Turbulent shear flow, however, is not amenable to a completely mathematical analysis. In order to proceed at all, the theory must depend on some empirical information. Because of the complexity of the flow

and the difficulty in measuring turbulent quantities, especially the shear stress, this empirical information is the essential difficulty in any analysis. Since there are slight differences in each case, such as irregularities in the wall, an average value of turbulent quantities can only be expected to hold within limits. In an adverse pressure gradient these difficulties are greatly amplified. Near separation the pressure is affected by the boundary layer, which is in turn critically dependent upon the pressure.

It should be emphasized that boundary layer theory alone can only be used up to separation, and because of the approximations cannot be very reliable in this region. For this reason, separation is not always predictable from boundary layer calculations, and a study of separated flow must include the geometry.

Even in the face of all these difficulties, the behavior of a turbulent boundary layer does appear to be predictable within limits. A large amount of work has been done in developing empirical methods of predicting this behavior, and undoubtedly more will be done in the future. Just how useful these methods are at present is largely a matter of opinion, but it can hardly be doubted that more work is needed. After a somewhat critical discussion concerning the present theories, Clauser[1] concludes that "the field is still wide open for the advent of a reliable method for predicting the behavior of turbulent layers under the influence of pressure gradients".

In attempting to improve the existing methods, however, it must be realized that some assumptions or empirical correlations must be made. Improvements can only be made through these assumptions, which are limited by the present understanding of turbulent shear flow. But it is quite likely that some improvements can be made without a great deal more quantitative knowledge of the mechanism that is really involved.

Perhaps what is even more desirable at this point is some idea of just how reliable such approximate methods are. Does their reliability justify their use in applications, or should designers continue to use somewhat conservative rules, such as the maximum lift coefficient for airfoils and the pressure rise for diffusers?

The objective of the present work, then, will be to examine just what assumptions must be made, improve them as far as possible, estimate the uncertainty involved, and finally, determine to what extent this uncertainty affects the final result.

II. REVIEW OF THE PROBLEM

Because of the complexity of turbulent flow, it is convenient to separate the velocity into mean and fluctuating components, as suggested by O. Reynolds. In the two-dimensional case the component of velocity parallel to the wall is written

$$u(x, y, t) = \bar{u}(x, y) + u'(x, y, t) \qquad (1)$$

where

$$\bar{u} = \frac{1}{2T} \int_{-T}^{T} u\,dt \qquad \text{and} \qquad \int_{-T}^{T} u'\,dt = 0$$

and similarly the component of velocity perpendicular to the wall

$$v(x, y, t) = \bar{v}(x, y) + v'(x, y, t) \qquad (2)$$

For convenience the bar is omitted from the mean, or time average, components, which are then written as simply u and v.

Substituting these velocities into the equations of motion and averaging with respect to time results in additional terms, which are the Reynolds stresses. The additional terms are, unfortunately, unknown with no further equations. This fundamental difficulty has so far limited the theoretical approach to turbulent flow, and forced the analysis to rely on experimental results.

(a) Basic Equations

The derivation of the turbulent boundary layer equations can be found in many books dealing with the subject (Refs. 2 - 7) so they will simply be listed here in their two-dimensional form.

x-momentum

$$u\frac{\partial u}{\partial x} + v\frac{\partial u}{\partial y} = -\frac{1}{\rho}\frac{\partial p}{\partial x} + \nu\frac{\partial^2 u}{\partial y^2} - \frac{\partial \overline{u'^2}}{\partial x} - \frac{\partial \overline{u'v'}}{\partial y} \qquad (3)$$

y-momentum

$$0 = -\frac{1}{\rho}\frac{\partial p}{\partial y} - \frac{\partial \overline{v'^2}}{\partial y} \qquad (4)$$

continuity

$$\frac{\partial u}{\partial x} + \frac{\partial v}{\partial y} = 0 \qquad (5)$$

where $\rho\overline{u'^2}$, $\rho\overline{v'^2}$ and $\rho\overline{u'v'}$ are the Reynolds stresses. The term $\rho\overline{u'^2}$ is the average flow of x-momentum, due to the turbulent motion, through a surface normal to the x-direction and is therefore interpreted as a normal stress. The term $\rho\overline{u'v'}$ is the flow of x-momentum through a surface parallel to the x-direction and is interpreted as a tangential, or shear stress.

The Reynolds normal stress is relatively small compared to the other terms in equation (3) and is usually neglected. (The importance of the normal stress will be discussed in part (d).) In this case the pressure can be assumed constant across the thin boundary layer, at least when the longitudinal curvature is small. Except in the viscous region very near the wall, the term $\nu\,\partial^2 u/\partial y^2$ is also relatively small.

Since the details of the turbulent flow are extremely complicated and the Reynolds stresses are unknown, it is usually advantageous to integrate equation (3) across the boundary layer. Neglecting the normal stress for the present, equation (3) can be integrated (see Refs. 2 and 3 for example).

$$\frac{\partial}{\partial x}\int_0^\delta \rho u^2 dy - U\frac{\partial}{\partial x}\int_0^\delta \rho u dy = -\delta\frac{dp}{dx} - \tau_w \qquad (6)$$

The usual boundary layer parameters are defined:

momentum thickness

$$\theta = \int_0^\delta \left[\frac{u}{U} - \left(\frac{u}{U}\right)^2\right] dy \qquad (7)$$

displacement thickness

$$\delta^* = \int_0^\delta \left(1 - \frac{u}{U}\right) dy \qquad (8)$$

shape factor

$$H = \delta^*/\theta \qquad (9)$$

friction coefficient

$$c_f = \frac{\tau_w}{\frac{1}{2}\rho U^2} \qquad (10)$$

The pressure may be written in terms of the free stream velocity by use of the Bernoulli equation.

$$p + \frac{1}{2}\rho U^2 = \text{constant}$$

or

$$-\frac{1}{\rho}\frac{dp}{dx} = U\frac{dU}{dx} \qquad (11)$$

Then, with the above definitions, equation (6) can be reduced to

$$\frac{d\theta}{dx} + (H + 2)\frac{\theta}{U}\frac{dU}{dx} = \frac{c_f}{2} \qquad (12)$$

Equation (12), however, contains three unknowns and does not enable one to calculate the shape of the velocity profile, which is of primary importance in an adverse pressure gradient. In order to proceed past this point, other equations must be determined either empirically or from the partial differenctial equation (3). There are several methods of obtaining further equations from equation (3), three of which will be listed here:

1) by taking moments in u or y, i.e. by multiplying equation (3) by $u^n y^m$ and integrating across the boundary layer. (This general approach is outlined in Ref. 8.) The zeroth moment, n = 0, m = 0, is the usual momentum integral equation (6) or (12). The first moments, n = 1, m = 0 and n = 0, m = 1, which result in the energy and moment of momentum equations, respectively, are also of primary importance. The energy equation obtained in this manner can be simplified to (Ref. 3)

$$\frac{1}{U^3}\frac{d}{dx}(U^3\delta^{**}) = 2\int_0^\delta \frac{\tau}{\rho U^2}\frac{\partial}{\partial y}\left(\frac{u}{U}\right)dy \qquad (13)$$

where

$$\delta^{**} = \int_0^\delta \frac{u}{U}\left[1 - \left(\frac{u}{U}\right)^2\right]dy \quad \text{(energy thickness)} \qquad (14)$$

2) by dividing the boundary layer into strips and integrating equation (3) across each strip

3) by satisfying equation (3) at certain points within the boundary layer.

In all of these methods the value of the turbulent shear stress within the boundary layer is necessary, as would be expected since it is the rate of transfer of momentum to the inner layers.

(b) Approximate Calculation Methods

Several methods of predicting the behavior of a turbulent boundary layer in an adverse pressure gradient have been proposed (Refs. 8 - 30). No attempt will be made to describe each of these methods individually here, but rather a summary of the assumptions on which they are based. (A comparison of some of the methods is given in Refs. 9 and 10.)

Almost all of the methods so far proposed make use of the momentum integral equation (12), or at least some variation of it. The problem then remains of obtaining further relations for the skin friction and shape factor.

The skin friction in an adverse pressure gradient is somewhat uncertain, but several empirical relations exist (Refs. 31 - 33, for example). One of the best known and perhaps most reliable skin friction equations for an adverse pressure gradient is that suggested by Ludwieg and Tillmann[33].

$$c_f = 0.246\, R_\theta^{-.268}\, 10^{-.678H} \tag{15}$$

By making two simplifying assumptions which may partly compensate for each other, equation (12) can be integrated. Since H only varies from approximately 1.3 to 2.5 for a turbulent boundary layer, $H + 2$ may be regarded as a constant in the integration. And, since the skin friction is usually unimportant in an adverse pressure gradient, an approximate flat plate equation may be used

$$c_f = \text{constant} \cdot R_\theta^{-1/n} \tag{16}$$

Then, equation (12) can be integrated (see Ref. 3)

$$\theta \left(\frac{U\theta}{\nu}\right)^{1/n} = \frac{1}{U^b}\left[C + a\int_{x_1}^{x} U^b dx\right] \tag{17}$$

where a, b and n are constants, usually taken as approximately 0.016, 4.0 and 4, respectively. C is the constant of integration.

It has been found (Refs. 13 and 14) that, if the pressure gradient is sufficiently severe, reasonable results can be obtained with the approximate relation

$$\frac{\theta}{\theta_1} = \left(\frac{U_1}{U}\right)^c \tag{18}$$

where c is an empirical constant, approximately 4.8 or 5.

In general, equation (12) and the preceding simplifications agree reasonably well with experiments, except possibly near separation. Where agreement is not good, several authors (Refs. 28, 34 - 39) have explained the discrepancy as the effect of normal stress or three-dimensional flow (see part (d)).

In order to predict the shape of the velocity profile or separation, however, some further relation is needed. It is here that the methods differ and agreement with experiment is no longer reliable.

Several attempts (Refs. 11 and 12) have been made to develop theories based on the form parameter

$$\Gamma = R_\theta^{1/n} \frac{\theta}{U} \frac{dU}{dx} \tag{19}$$

which corresponds to the Pohlhausen parameter for laminar flow (see Ref. 3). The assumption here is that the shape of the velocity profile is only a function of local conditions, which is not true if these conditions are changing rapidly, even in laminar flow. In special cases and where the conditions change very slowly, however, a local parameter such as Γ might be of value. But as suggested by Prandtl[40] one would in general expect the rate of change in the velocity profile, not the profile itself, to be related to Γ.

Most methods of predicting turbulent boundary layer behavior make use of the assumption that the velocity profiles form a one parameter family, which has been verified reasonably well by experiments. The profiles are usually characterized by the shape factor, H, as a parameter.

$$\frac{u}{U} = f(\eta, H) \qquad \eta = y/\delta \tag{20}$$

The shape factor varies from approximately 1.4 for zero pressure gradient to 2.5 near separation, for turbulent boundary layers. Typical profiles are shown in the following figure.

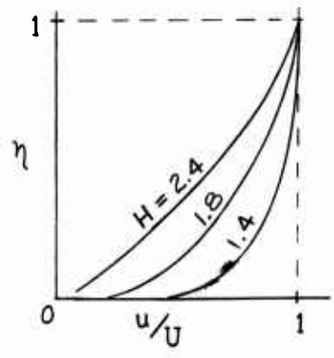

The problem then reduces to one of finding an equation for H or its derivative. Many of the shape factor equations that have been suggested can be written in the form: (Ref. 10)

$$\theta \frac{dH}{dx} = g_1(R_\theta , H) \frac{\theta}{U} \frac{dU}{dx} + g_2(R_\theta , H) \tag{21}$$

Equation (21) may be strictly empirical, or it can be derived from equation (3) as outlined in the preceding section, with an empirical relation for the turbulent shear stress.

The most usual assumption for the velocity profile is the power-law;

$$\frac{u}{U} = (\eta)^{1/n} \tag{22}$$

where, from the definition of H, equation (9)

$$n = \frac{2}{H - 1} \tag{23}$$

With this assumption for the velocity profile, the shape factor equation (21), based on the first moments of equation (3), may be derived; (see Ref. 8)

<u>energy</u>

$$\theta \frac{dH}{dx} = - H(H - 1)(3H - 1) \frac{\theta}{U} \frac{dU}{dx} + (3H - 1) \left[H \frac{c_f}{2} - \frac{(3H - 1)}{2} \times \int_0^\delta \frac{\tau}{\rho U^2} \frac{\partial}{\partial y} \left(\frac{u}{U}\right) dy \right] \tag{24}$$

<u>moment of momentum</u>

$$\theta \frac{dH}{dx} = - \frac{H(H + 1)(H^2 - 1)}{2} \frac{\theta}{U} \frac{dU}{dx} + (H^2 - 1) \left[H \frac{c_f}{2} - (H + 1) \int_0^\delta \frac{\tau}{\rho U^2} \, dy \right] \tag{25}$$

The physical significiance of the terms in equation (21) now becomes apparent. The first term on the right represents the pressure force, which acts with equal magnitude across the boundary layer and tends to move it toward separation. The second term, g_2, represents

the shear forces which, in an adverse pressure gradient, transfer momentum to the inner layers and tend to delay separation. If the pressure gradient is sufficiently severe, the shear forces are unimportant except very near the surface and g_2 is not important in equation (21) (Ref. 24). On the other hand, when the shape is not changing, dH = 0, the two terms are equal.

In general, equation (21) depends on three factors;

1) the velocity profile assumption,

2) the method of derivation,

3) an empirical relation for the shear stress.

It is generally agreed that the greatest uncertainty is involved with the turbulent shear stress, so this factor will be discussed in detail later. The effect of the first two factors can be seen by comparing the functions g_1 and g_2. Figure 1a shows the function g_1 based on the power-law profile for the energy equation (24), the moment of momentum equation (25), and an equation derived by integrating (3) across the inner half of the boundary layer. Figure 1b shows g_1 based on the moment of momentum for three velocity profile assumptions.

1) power-law

2) linear, $u/U = a + b\eta$

3) experimental profiles of Ref. 41.

The function g_2 depends on the shear stress assumption which in turn depends on the method of derivation, but the effect of the velocity profiles can be compared for any derivation. For the moment of momentum g_2 can be written:

$$g_2 = h_1 \frac{\tau_w}{\rho U^2} - h_2 \int_0^1 \frac{\tau}{\rho U^2} \, d\eta \qquad (26)$$

The functions h_1 and h_2 are compared in Figure 2 for the three profiles.

To summarize briefly, most recent methods of predicting turbulent boundary layer behavior make use of the momentum integral equation (12) with an empirical equation for the skin friction. The boundary layer is then characterized by the shape factor, H, which is determined from an equation of the form (21). The shape factor equation involves some assumptions concerning the velocity profiles and the shear stress within the boundary layer.

(c) Turbulent Shear Stress

The shear stress within the boundary layer

$$\tau = \mu \frac{\partial u}{\partial y} - \rho \overline{u'v'} \tag{27}$$

has so far proved to be the most uncertain factor in predicting the behavior of turbulent boundary layers. It is this unknown quantity, along with the Reynolds normal stress, that forces any analysis to be only approximate.

One possible approach to the problem (Ref. 42) is to express the shear stress in the form

$$\frac{\tau}{\tau_w} = a + b\eta + c\eta^2 + d\eta^3 \tag{28}$$

where the coefficients are determined from the boundary conditions

$$\eta = 0 \qquad \tau = \tau_w \qquad \frac{\partial \tau}{\partial y} = \frac{\partial p}{\partial x} \text{ (from equation (3))}$$

$$\eta = 1 \qquad \tau = 0 \qquad \frac{\partial \tau}{\partial y} = 0$$

Then, equation (28) can be written

$$\frac{\tau}{\tau_w} = (1 - 3\eta^2 + 2\eta^3) + (\eta - 2\eta^2 + \eta^3) \frac{\delta}{\tau_w} \frac{\partial p}{\partial x} \tag{29}$$

Equation (29), however, assumes that the shear stress only depends on local conditions and, unless this is true of the velocity profile, implies that it is independent of the velocity gradient normal to the wall.

Perhaps the most usual approach is to define a turbulent, or eddy, viscosity as suggested by Boussinesq;

$$-\overline{u'v'} = \epsilon \frac{\partial u}{\partial y} \tag{30}$$

which corresponds to the kinematic viscosity in the laminar case. This definition, of course, simply replaces one unknown by another, but it is sometimes useful in making empirical generalizations about the shear stress.

The problem now remains of finding an expression for the eddy viscosity. If the turbulent shear stress is assumed constant near the wall and the velocity is logarithmic (see part (f)) then ϵ must be linear.

$$\epsilon = (\kappa u_\tau) y \tag{31}$$

For pipe flow and boundary layers in zero pressure gradients, it can be shown from the velocity profiles (see Refs. 3 and 6) that ϵ is approximately parabolic with distance from the wall.

$$\frac{\epsilon}{u_\tau \delta} = (1 - y^2) \text{ constant} \tag{32}$$

However, it has been found (Refs. 1, 3 and 43) that in many cases, such as free shear flows and the outer part of the boundary layer, reasonable results can be obtained with a very simple assumption of the form

$$\frac{\epsilon}{U\delta} = \text{constant} \tag{33}$$

In most of the approximate theories just described, an integrated value of the shear stress is needed, which may be obtained directly from experiments or by use of an expression for the eddy viscosity. The suggested values differ widely, so only two typical examples are listed here, corresponding to equations (24) and (25).

$$\int_0^\delta \frac{\tau}{\rho U^2} \frac{\partial}{\partial y}\left(\frac{u}{U}\right) dy = \frac{.56 \times 10^{-2}}{R_\theta^{1/6}} \quad \text{(Ref. 22)} \tag{34}$$

and

$$\frac{1}{\theta} \int_0^\delta \frac{\tau}{\rho U^2} dy = .044 \frac{H}{H+3} R_\theta^{-1/10} \quad \text{(Ref. 27)} \tag{35}$$

(d) Turbulent Normal Stress

In the derivation leading to equation (12) from equation (3) it was assumed that the Reynolds normal stresses

$$\frac{\partial \overline{u'^2}}{\partial x} \quad \text{and} \quad \frac{\partial \overline{v'^2}}{\partial y}$$

were small compared to the other terms and could be neglected. However, several authors (Refs. 28, 34 - 37) have questioned the validity of this assumption, especially near separation. Some discrepancies between equation (12) and experiments have been noted, which might be explained in part by the omission of the normal stress. Other investigators (Refs. 1 and 38) have contended that the discrepancies are due mainly to small amounts of three-dimensional flow.

If the $\overline{u'^2}$ term is left in equation (3) through the integration

$$\frac{1}{U^2} \int_o^\delta \frac{\partial \overline{u'^2}}{\partial x} \, dy$$

must be added to the right hand side of equation (12).

If the $\overline{v'^2}$ term is also considered, the y-momentum equation (4) must be used, which can be integrated.

$$p = p_o - \int_{y_o}^{y} \frac{\partial \overline{v'^2}}{\partial y} \, dy = p_o - \overline{v'^2} \qquad (36)$$

where p_o is the pressure outside the turbulent region.

The momentum integral equation corresponding to equation (12) can now be written (Ref. 4)

$$\frac{d\theta}{dx} + (H + 2) \frac{\theta}{U} \frac{dU}{dx} = \frac{c_f}{2} + \frac{1}{U^2} \int_o^\delta \frac{\partial}{\partial x} (\overline{u'^2} - \overline{v'^2}) \, dy \qquad (37)$$

In order to determine the importance of these additional terms, the experiments of Reference 41 have been compared in Figure 3. Here the calculated values are shown for equation (12) alone, with the correction for $\overline{u'^2}$ included, and for the complete equation (37).

Without intending any implication about the experimental data, the result of assuming an arbitrary small amount of three-dimensional flow is also shown in the figure. In this case the momentum integral equation can be written, for the line of symmetry, (see Ref. 56)

$$\frac{d\Theta}{dx} + (H + 2)\frac{\Theta}{U}\frac{dU}{dx} = \frac{c_f}{2} - \frac{1}{U^2}\int_0^{\delta} (U - u)\, u \frac{\partial \omega}{\partial z}\, dy \qquad (38)$$

where ω is the angle between the streamline and centerline. For the present purpose, it was assumed that $\partial\omega/\partial z$ is constant in the y-direction (1°/FT.) which is similar to an axisymmetric body with changing radius, or radial flow. In general, this assumption would not be true, but it gives some idea of the relative importance of the normal stresses and small amounts of three-dimensional flow.

The turbulent normal stress, like the shear stress, must be determined empirically. Two examples of the expressions that have been suggested are

$$\frac{1}{U^2}\int_0^{\delta} \frac{\partial \overline{u'^2}}{\partial x}\, dy = f\left(\Theta \frac{dH}{dx}\right) \qquad \text{(Ref. 28)} \qquad (39)$$

and

$$\frac{1}{U^2}\int_0^{\delta} \frac{\partial}{\partial x}\left(\overline{u'^2} - \overline{v'^2}\right) dy = \frac{k}{U^2}\frac{d}{dx}\left(\delta^* U^2\right) \qquad \text{(Ref. 36)} \qquad (40)$$

(e) Non-uniform Mean Flow

It is usually implied in the use of two-dimensional equations of motion that the time mean flow is in fact two-dimensional, i.e. uniform in the z-direction. It is known (Refs. 56 and 57) that streaks or longitudinal vortices do exist, even when the overall average flow is two-dimensional. If these irregularities move about randomly, no error arises from the use of two-dimensional equations. On the other hand, if they remain fixed because of irregularities in the surface or approaching flow, additional terms occur in the equations.

Following the method of Reference 56, these additional terms can be derived as follows. The total velocity may be divided into a space-time mean, which corresponds to the usual time mean, the usual time fluctuating velocity, and a space perturbation.

$$u(x, y, x) = \bar{u}(x, y) + u'(x, y, z, t) + u''(x, y, z) \quad (41)$$

where

$$\bar{u} = \frac{1}{4TZ} \int_{-Z}^{Z} \int_{-T}^{T} u \, dt \, dz$$

$$\int_{-T}^{T} u' \, dt = 0 \qquad \text{and} \qquad \int_{-Z}^{Z} u'' \, dz = 0$$

Similarly for the v-component,

$$v(x, y, z, t) = \bar{v}(x, y) + v'(x, y, z, t) + v''(x, y, z) \quad (42)$$

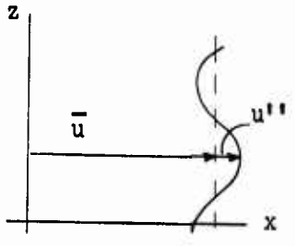

Then, by using these velocities in the equations of motion, the following terms appear in equation (3) instead of the usual Reynolds stresses.

$$\frac{\partial}{\partial x} (\overline{u'^2} + \overline{u''^2}) \quad \text{and} \quad \frac{\partial}{\partial y} (\overline{u'v'} + \overline{u''v''})$$

In some cases, such as behind a vortex generator or a strut, these additional terms may be very important. In the usual adverse pressure gradient, their importance is still uncertain. Since no quantitative results have been published and none could be measured in the present experiments, these terms must be neglected, at least for the present. Compared with the other uncertainties involved, this effect is probably not important.

(f) Separation

The ultimate goal in attempting to predict the behavior of the turbulent boundary layer is, of course, the ability to predict separation, or stall.

Several attempts have been made to develop separation criteria of the form

$$\Gamma = R_\theta^{1/n} \frac{\theta}{U} \frac{dU}{dx} = \text{constant (at separation)} \qquad (41)$$

The impossibility of determining a universally valid constant from the experimental data is shown in Figure 4. However, such a criterion might be useful in special cases and as a lower limit, below which separation would not occur.

In most of the approximate methods, separation is assumed to occur when the shape factor reaches a certain value, for example $H = 2.5$. However, due to the approximations, these methods are not very reliable for large values of H. In many cases separation takes place very suddenly, and the uncertainty in the shape factor is no problem. When the pressure rise is very gradual for some distance upstream of separation, the predictions usually fail (see Ref. 9).

Some recent objections have been given to the usual conception of stall (Ref. 44) and the implication that boundary layer theory alone is sufficient to predict it. Turbulent separation is, in fact, a very complicated process and usually takes place over a somewhat unsteady region. It is clear that a thorough investigation of separated flow must include the particular configuration. However, it can hardly be denied that the behavior of the boundary layer is a necessary part, which can be treated independently, within limits.

(g) The Wall and Wake Laws

In addition to the prediction methods described above, a large amount of effort has been expended in obtaining useful correlations of the mean quantities in turbulent flow. The power-law discussed earlier is one example, which probably stems from the observation that in the absence of a pressure gradient the velocity near a surface can be approximated

by a 1/7 power. It was later extended to the case of a pressure gradient, with some experimental justification, by assuming a variable power.

Perhaps the most important correlations of this type are known as the "law of the wall" and "law of the wake". These laws and their implications have been thoroughly discussed by several authors, especially References 51, 52, and 53, so only a brief outline is attempted here.

If it is assumed that, in the absence of a pressure gradient, the flow near a solid surface is only dependent on local conditions, then dimensional arguments lead to the conclusion.

$$\frac{u}{u_\tau} = \phi\left(\frac{y u_\tau}{\nu}\right) \tag{42}$$

where $u_\tau = \sqrt{\tau_w/\rho}$ is the friction velocity.

Except for a thin viscous sublayer, it has been found empirically and by arguments that will be discussed later that equation (42) can be written

$$\frac{u}{u_\tau} = \frac{1}{\kappa} \log\left(\frac{y u_\tau}{\nu}\right) + B \tag{43}$$

where κ and B are empirical constants, The values that have been suggested vary slightly, but those listed in Reference 51 are .40 and 5.1, respectively.

One very important inference, based on experimental observations (Ref. 33) is that equation (43) holds even in the presence of a pressure gradient. Some theoretical work has been done in determining the limits of the wall law, but because of the unknown eddy viscosity, nothing really conclusive can be said. The arguments leading to equation (42) are based on the fact that near the wall the shear stress is very large compared to the inertia and pressure force. In the case of a pressure gradient, the shear stress is large compared to the pressure force for only a limited value of y.

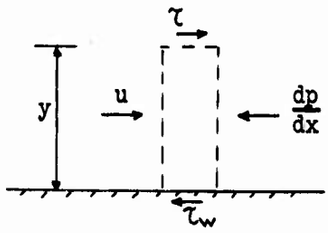

For a balance between pressure and shear forces

$$\frac{\tau}{\tau_w} = 1 + \lambda y^+ \tag{44}$$

where $y^+ = \left(\frac{y u_\tau}{\nu}\right)$ and $\lambda = \frac{\nu}{\tau_w u_\tau}\frac{dp}{dx}$

and by definition $$\frac{\tau}{\tau_w} = \left(\frac{\epsilon}{\nu} + 1\right)\frac{\partial u/u_\tau}{\partial y^+}$$

In order to integrate equation (44) for the velocity, some assumption must be made about the eddy viscosity. In zero pressure gradient, assuming $\tau = \tau_w$

$$\frac{1}{\frac{\epsilon}{\nu} + 1} = \phi'(y^+) \tag{45}$$

where ϕ is the universal function. If it is assumed that equation (45) is valid for an adverse pressure gradient, the velocity can be written

$$\frac{u}{u_\tau} = \phi(y^+) + \lambda \int_0^{y^+} y^+ \phi'(y^+)\, dy^+ \tag{46}$$

Since the turbulent viscosity would not be expected to approach zero even when τ_w vanishes, Ferarri[54] assumes

$$\epsilon = k\sqrt{\frac{\tau}{\rho}}\, y = k\, y \sqrt{\frac{\tau_w}{\rho} + \frac{dp}{dx}\frac{y}{\rho}} \tag{47}$$

which decreases the effect of the pressure on the velocity.

The law of the wall from Reference 51 is shown in Figure 5, along with the possible corrections for pressure.

The wake law, or velocity defect, is usually written in the form

$$\frac{u - U}{u_\tau} = \psi(\Pi, \eta) \tag{48}$$

where Π is only a function of x.

If equations (42) and (48) are assumed to agree in some overlapping region, then a logarithmic relation follows immediately. By combining the two laws, Coles[53] writes for the entire boundary layer

$$\frac{u}{u_\tau} = \frac{1}{\kappa} \log \frac{y u_\tau}{\nu} + B + \frac{\Pi}{\kappa} w(\eta) \qquad (49)$$

where w is a universal wake function. The function, w, as determined by Coles from a large amount of experimental data, is shown in Figure 5 with the approximation,

$$w = 2(3\eta^2 - 2\eta^3) \qquad (50)$$

The wake parameter, Π, is an unknown function of the Reynolds number and pressure gradient but is independent of y, the distance from the wall. For zero pressure gradient $\Pi = .55$, except at low Reynolds numbers where it vanishes.

(h) Special Cases

The difficulties involved in a general approach to the problem have led to the investigation of special cases, two of which are the equilibrium layer and the boundary layer with zero skin friction.

The equilibrium layer (Refs. 1, 30, 58 and 59) is one that has developed through a region of unchanging conditions, i.e., a constant ratio of the shear and pressure forces. The velocity profiles are then similar when plotted as

$$\frac{u - U}{u_\tau} \quad \text{v.s.} \quad \eta$$

which corresponds to a constant wake parameter, Π, in the preceding section. The boundary layer in zero pressure gradient is one example of the equilibrium layer.

The boundary layer with zero, or negligible, shear stress has also been investigated (Refs. 29, 50, 60 and 61). In this case, the flow is decelerated as rapidly as possible without causing separation. After a

sufficient length of development, the boundary layer should approach equilibrium.

These special cases represent definite conditions to which the boundary layer is subjected, and for which the response can be observed. By making certain assumptions concerning the velocity and turbulent shear stress, this response might be predicted. Then by generalizing these assumptions, the response to an arbitrary pressure gradient might also be predicted.

(i) Evaluation of Existing Theories

Since there are no exact solutions for the turbulent boundary layer, an ultimate evaluation of the existing theories must depend on experiments. Some of these methods have been compared with experiments other than those on which they were based (see Figures 7a, 7b), with the general conclusion that more work is needed. However, it is not the purpose of the present review to evaluate each of the several methods individually, but to examine the basic assumptions that must be made.

One of the basic assumptions that can be improved in most methods is the velocity profiles. The power-law, or any one-parameter family, becomes very approximate in an adverse pressure gradient. The shape factor varies with the Reynolds number even at constant pressure. It is usually argued that this assumption is not critical, and a simple one is justified in order to facilitate hand calculations. However, this restriction is not necessary, and a computer solution may even be desirable.

Undoubtedly, one of the main difficulties with the existing methods is the turbulent shear stress. Although this may always be the case, the previous assumptions can definitely be improved. It is generally agreed that the shear stress is the most critical part of the analysis, but relatively little work has been done in developing a reliable correlation.

However, the main objection to the present situation is not the approximate methods, but the failure to fully examine their limitations. Although the turbulent shear stress is (and must remain) somewhat uncertain, its effect has not been examined quantitatively. In addition, the limit to which these methods should be relied upon in approaching separation has hardly been considered at all.

The purpose of the present experiments and analysis, then, can be divided into three factors

1) to improve the necessary assumptions as far as possible

2) to develop a calculation method, using these assumptions, that can be easily applied

3) to examine the limitations that any approximate method must have with the present uncertainty in turbulent shear flow.

III. EXPERIMENTAL PROGRAM

A fairly large number of experiments on the turbulent boundary layer in an adverse pressure gradient have been published (Refs. 1, 17, 20, 35, 41, 46 - 50). However, most of the experiments were limited to one configuration and one pressure distribution. Differences in behavior from one experiment to another in these cases may be largely due to the peculiarities of the apparatus. In many of the experiments there is at least some uncertainty concerning three-dimensional flow. In some cases a reasonably large aspect ratio of channel width to height was reported, but perhaps even more important is the width of the channel to the length of pressure rise. Although it is generally agreed that the most critical part of the approximate methods is the turbulent shear stress, relatively little experimental data exists.

For these reasons, an experimental investigation has been carried out, concentrating on three main objectives:

1) obtaining data for several pressure distributions on one apparatus

2) obtaining data as free as possible from three-dimensional flow (or with control of three-dimensional effects)

3) obtaining data for the turbulent shear stress.

(a) Apparatus and Equipment

A photograph of the apparatus and equipment is shown in Figure 8a and a schematic diagram in Figure 8b. The test section consists of a 6 inch plastic cylinder concentric with a 15 inch diameter porous metal cylinder. Air is supplied by a 6000 CFM axial flow fan into a 7 foot long chamber, then through a honeycomb and three screens, and finally accelerated to a approximately 100 $\frac{\text{ft.}}{\text{sec.}}$ at the entrance of the working section.

An adjustable end plate in the annulus causes the flow to diffuse out through the porous metal and creates the adverse pressure gradient. It can be removed for comparison with zero pressure gradient. The boundary layer to be studied grows along the plastic cylinder and separates somewhere in front of the end plate. The pressure distribution can be adjusted as desired by symmetric strips on the porous cylinder, which can be moved to any position or removed entirely. The strips can also be placed on one side only to create a three-dimensional flow.

The static pressure is taken by a row of static taps spaced 2 inches apart along the cylinder and at three positions on the bottom and sides. The plastic cylinder can be rotated to any angular position in order to check the pressure variation around the test section. The static taps are 1/8 inch brass rods inserted into the plastic and ground flush with the surface, with .030 inch holes. The static pressures are read on a 26 tube inclined manometer board on which the pressure distribution can be observed directly.

The mean velocity was measured by total head tubes of various sizes from .020 to .080 inch outside diameter, using the static pressure from the wall taps. The probes were mounted on a micrometer traversing mechanism for taking the velocity profiles and could be inserted through the porous cylinder at any desired position.

(b) Hot-wire Equipment

The hot-wire equipment consisted mainly of two transistorized, constant temperature amplifiers and linearizers manufactured by Leslie T. Miller, of Baltimore, Maryland. The units were mounted on a single chassis for making the $\overline{u'v'}$ measurements. The wires were .00015 inch diameter tungsten, copper plated on each end with a bare section .060 inches long. The wires were soldered onto needles spaced about 1/8 inch apart and mounted on a steel tube that could be used with the micrometer traversing mechanism.

Power was supplied to the hot-wire amplifiers by two 6 volt wet-cell batteries. The D. C. voltage output was read on a Heathkit VTM and fluctuating voltage on an Electronics Instrument RMS meter. The signal was monitored on a Dumont Model 304-A oscilloscope and the low frequencies recorded on a Sandborn Model 300B recorder. The energy spectrum was taken with a Hewlett-Packard M302A wave analyzer.

(c) Experimental Methods

The static pressure taps were checked in zero pressure gradient for sensitivity to flow and found to check within 1 percent of the dynamic head. The inclined manometer could be read within $\pm$ .004 inches of water.

The flow was checked for symmetry by rotating the pressure taps to different angles, observing the 'line' of separation, and by observing the flow direction. In no cases could three-dimensional flow be detected.

A small calibrating tunnel was used with the hot-wire instruments. For the single wire, the procedure was quite straight forward, and the mean values checked reasonably well with the pitot measurements. The cross-wire used for making $\overline{u'v'}$ measurements, however, was extremely difficult to calibrate. The wires were first calibrated individually in the small tunnel, taking care to make the response as linear and as nearly the same for both wires as possible. The probe was then placed in the apparatus and checked in the free stream at two speeds. A second calibration was made by removing the end plate and taking the RMS voltage near the wall in zero pressure gradient, which should agree with the skin friction. The skin friction in this case could be determined by comparing the mean velocity profile with the 'wall law'. Then, by assuming

$$\overline{u'v'} = \text{constant} \cdot \text{RMS}$$

the constant could be determined. The constants determined in both ways usually differed by approximately $\pm$ 5 percent; if more than 10 per cent the process was repeated. The difficulties were due mainly to the response of the wires not being linear and equal, drift of the electronic system, and improper alignment. It was felt that these errors were minimized by calibration in the apparatus at zero pressure gradient, so the value found in this way was used.

(d) Experimental Results

Some typical experimental results, taken with the above apparatus, as shown in Figures 9 - 14. The mean quantities include the pressure distribution in terms of the free stream velocity and the ususal parameters, θ and H, which were determined from the measured velocity profiles. These values are shown as a function of x, the distance along the cylinder starting from the first pressure tap, which was approximately the point of minimum pressure.

Three basically different pressure distributions are shown in Figure 9, which differ widely in pressure rise to separation. The advantage of early deceleration may be explained by the greater ability of a thin boundary layer to transfer momentum to the retarded flow by turbulent shear stress. The limitations of boundary layer theory become apparent in pressure distribution (3), where the pressure continues to rise for some distance beyond the beginning of separation.

Two linear pressure distributions are shown in Figure 10 (No. 2 is the same as in Fig. 9). In this case the x-dimension is divided by the starting momentum thickness, θ_1. These curves show experimentally the effect of an increase in the relative length, L/θ_1, on the pressure rise to separation.

Figure 11 shows the result of a sudden deceleration followed by a region of constant pressure. Some idea of the length required for the boundary layer to respond to a change in the pressure gradient can be obtained from this result, as well as the limitations of a form parameter based on local conditions.

The turbulent quantities, taken from hot-wire measurements, are shown in Figures 12 - 14. Figure 12 shows the turbulent intensity, $\overline{u'^2}$, as a function of distance from the wall. The values are given for three positions along the cylinder and were taken in the linear pressure distribution (2). The corresponding measurements of the turbulent shear stress, $\overline{u'v'}$, are shown in Figure 13. Finally, the turbulent energy spectrum was taken for a few cases, two of which are shown in Figure 14.

IV. ANALYSIS

The genral case of the approach that will be used here may be outlined by first writing the velocity in the form

$$\frac{u}{U} = \phi_1(\eta) + \alpha\phi_2(\eta) + \beta\phi_3(\eta) + \delta\phi_4(\eta) + \ldots . \qquad (51)$$

where $\eta = y/\delta$, $\phi(\eta)$ are $m + 1$ prescribed functions of η, and $\alpha, \beta, \gamma, \ldots$ are m parameters. In general, by making a wise choice for the $\phi(\eta)$, fewer are needed.

Then by any of the methods mentioned in Section II, $m + 1$ ordinary differential equations can be derived for δ and the m parameters. With the above velocity profiles these equations can be reduced to the form

$$d\delta = F_1(\delta, \alpha, B, \ldots, \tau, U)\, dx \qquad (52)$$

$$d\alpha = F_2(\quad " \qquad\qquad ")\, dx$$

$$d\beta = F_3(\quad " \qquad\qquad ")\, dx$$

$$d\gamma = F_4(\quad " \qquad\qquad ")\, dx$$

Then, with starting values of δ and the m parameters, given U as a function of x, and a method of determining the shear stress, τ, the equations can be solved by a numerical stepwise procedure.

In the laminar case

$$\tau = \mu \frac{\partial u}{\partial y} = \mu\, U/\delta\ f(\alpha, \beta, \gamma, \ldots) \qquad (53)$$

Then by taking a sufficient number of parameters, equations (52) can be solved as accurately as desired (Ref. 62).

In turbulent flow, however, the shear stress must be approximated from experiemental data and is the most uncertain part of the analysis. Using more parameters necessitates more assumptions about the shear stress and makes the solution more dependent upon it. The object, then, is to choose the functions in equation (51) so that only one or two parameters are needed.

When a more reliable approximation for the shear stress becomes available, through more experimental data and perhaps a better understanding of the flow, it might be advantageous to use more parameters.

(a) Velocity profiles

As mentioned in Section II, the most usual assumption for the velocity profiles is the power-law, but many others have been used. It is generally argued that this assumption is not too critical, and simple ones are justified. While this is indeed the case, it was felt that the velocity profiles should be improved as far as possible before examining the effect of the other approximations.

No one or two parameter family of velocity profiles could be expected to fit every possible case, but perhaps the best so far proposed is that of Coles (Ref. 53).

$$\frac{u}{u_\tau} = \frac{1}{\kappa} \log\left(\frac{y u_\tau}{\nu}\right) + B + \frac{\Pi}{\kappa} w(\eta) \qquad \begin{matrix}(49)\\ \text{repeated}\end{matrix}$$

where $\eta = y/\delta$, $\kappa = .40$, $B = 5.1$. By rearranging and redefining the variables, equation (49) can be written in the form (51). At $\eta = 1$, $u = U$. Then

$$\frac{U}{u_\tau} = \frac{1}{\kappa} \log\left(\frac{\delta u_\tau}{\nu}\right) + B + \frac{\Pi}{\kappa} w(1) \qquad (54)$$

Subtracting equation (54) from (49)

$$\frac{u - U}{u_\tau} = \frac{1}{\kappa} \log(\eta) + \frac{\Pi}{\kappa}\left[w(\eta) - w(1)\right] \qquad (55)$$

But
$$u_\tau = \sqrt{\frac{\tau_w}{\rho}} = \sqrt{\frac{c_f}{2}} \cdot U \qquad (56)$$

Letting
$$\alpha = \frac{1}{\kappa}\sqrt{\frac{c_f}{2}} = \frac{1}{\kappa}\frac{u_\tau}{U} \qquad (57)$$

$$\beta = -2\Pi\alpha$$

and using the approximation for $w(\eta)$

$$w = 2(3\eta^2 - 2\eta^3) \qquad \begin{matrix}(50)\\ \text{repeated}\end{matrix}$$

Equation (49) can finally be written

$$\frac{u}{U} = 1 + \alpha \log \eta + \beta(1 - 3\eta^2 + 2\eta^3) \qquad (58)$$

With the above definitions, equation (54) can be written

$$1 = \alpha \log\left(\frac{\delta U}{\nu} \cdot K \cdot \alpha\right) + \alpha B + \beta$$

or
$$\beta = \alpha\left[\log\left(\alpha R_\delta\right) + 1.1237\right] - 1 \qquad (59)$$

These equations (58) and (59) constitute a two parameter family, but with the parameters related by the Reynolds number. Therefore only two further equations are needed for the unknowns α and δ. The profiles are shown in Figure 15 for one Reynolds number.

Equation (54) and (59) are an implicit expression for the skin friction, c_f, in terms of the shape of the velocity profiles and the Reynolds number. This relation is shown in Figure 16, compared with the Ludwieg-Tillmann equation.

(b) Momentum Integral Equations

With the above velocity profiles, two further equations are needed. The first is obtained by integrating equation (3) across the boundary layer, from $y = 0$ to δ. The result is, of course, the usual momentum integral equation, which in this case can be written (see Appendix A)

$$f_5 \frac{d\delta}{dx} + f_6 \frac{d\alpha}{dx} + f_7 \frac{d\beta}{dx} = f_8 \qquad (60)$$

Since the skin friction is related to α by equation (57) no further unknowns are involved in equation (60).

Any of the methods mentioned in Section II might be used to derive a second equation. In general, there have been no really convincing arguments as to which method is most reliable. The first two methods might be preferable, especially for turbulent flow, since they involve integrated quantities rather than values at a point. With the above assumption for the velocity profiles, the method of dividing the boundary layer into strips is by far the simplest. For this reason it is used in the present analysis.

Then, in order to derive a second equation, the momentum integral is satisfied over the inner half of the boundary layer. Integrating to $\eta = .5$ is arbitrary, but it seems reasonable when using two equations to take approximately half of the boundary layer. This choice should not be critical as long as values not too close to 0 or 1 are used. A value of $\eta = .4$ was also tried, with almost identical results.

The integral of equation (3) from $y = 0$ to y can be written

$$u(y)\frac{\partial}{\partial x}\int_0^y u\,dy - \frac{\partial}{\partial x}\int_0^y u^2 dy = \frac{y}{\rho}\frac{dp}{dx} + \frac{\tau_w - \tau(y)}{\rho} + \frac{1}{U^2}\int_0^y \frac{\partial}{\partial x}(\overline{u'^2} - \overline{v'^2})dy \qquad (61)$$

Evaluating equation (61) at $\eta = .5$ with the above velocity profiles results in the second equation (see Appendix A).

$$f_9\frac{d\delta}{dx} + f_{10}\frac{d\alpha}{dx} + f_{11}\frac{d\beta}{dx} = f_{12} \qquad (62)$$

The shear stress, $\tau(y)$, which represents the transfer of momentum due to the turbulent mixing between the two halves of the boundary layer, is included in the function f_{12}.

(c) Turbulent Shear Stress

As mentioned earlier, the turbulent shear stress is the point where any analysis must rely on experimental results, at least with the present understanding of turbulent shear flow. Since these results are not very conclusive, it is also the point where the most uncertainty is introduced into the analysis.

For lack of a better approach, the eddy viscosity is again defined

$$\frac{\tau}{\rho U^2} = \frac{\epsilon}{U\delta}\frac{\partial(u/U)}{\partial\eta} \qquad (63)$$

As a first approximation, it might be assumed that the eddy viscosity can be written

$$\frac{\epsilon}{U\delta} = f(R_\delta, \eta) \qquad (64)$$

Since for the present calculation method, the shear stress is only needed at $\eta = .5$

$$\left(\frac{\epsilon}{U\delta}\right)_{\eta=.5} = f(R_\delta) \tag{65}$$

Then by applying the momentum balance, equation (61), to the well established data for zero pressure gradient, the function $f(R\delta)$ can be determined. These results, which were based on the values of Π from Reference 63, can be approximated by

$$\frac{\epsilon}{U\delta} = \frac{.004}{\log R_\delta - 7.6} + .0013 \qquad \begin{matrix}\eta = .5 \\ (R_\delta \geq 5000)\end{matrix} \tag{66}$$

In an attempt to test the validity of the assumption leading to equation (66), that the eddy viscosity can be approximated by equation (64) regardless of the pressure gradient, some experimental values have been examined. The turbulent shear stress was determined by hot-wire measurements and by the momentum balance, equation (61). Since the shear stress in an adverse pressure gradient is usually a small difference between two large terms, the latter method is not very reliable, especially near separation. The eddy viscosity was then determined with the measured slope of the velocity profiles. Figure 17 shows these results compared with the zero pressure gradient data and equation (66).

It must be admitted that equation (66) is very approximate, but it gives reasonable results. The experimental evidence is not sufficiently conclusive to improve it, at least for the present.

(d) Turbulent Normal Stress

Like the shear stress, the turbulent normal stress, $\overline{u'^2}$ and $\overline{v'^2}$, must be determined from experimental results. In this case, however, the approximation is not important, and it is usually neglected entirely.

Although these terms are small, they do occur in the equations and have a slight effect on the calculations. For this reason they are

included in the present analysis. It was found, for the present purpose, that the limited data could be represented reasonably well by the following approximations.

$$\frac{1}{U^2}\int_0^{\delta}\frac{\partial}{\partial x}\left(\overline{u'^2}-\overline{v'^2}\right)dy = 2(.15-\alpha)^2\frac{\delta}{U}\frac{dU}{dx} \qquad (67)$$

$$\frac{1}{U^2}\int_0^{\delta}\frac{\partial}{\partial x}\left(\overline{u'^2}-\overline{v'^2}\right)dy = \frac{2}{3}(.15-\alpha)^2\frac{\delta}{U}\frac{dU}{dx} \qquad (68)$$

(e) Numerical Calculations

With the assumptions for the velocity profiles, equation (66), and the turbulent normal stress, equations (67 and 68), the simultaneous differential equations (60), (62) and (A-1) can be reduced to

$$\frac{d\delta}{dx} = F_1(\alpha, \beta, \delta, U)$$

$$\frac{d\alpha}{dx} = F_2(\alpha, \beta, \delta, U) \qquad (69)$$

β is determined from equation (59).

Given starting values of δ and α, and U as a function of x, equations (69) can now be solved in a numerical, stepwise procedure. The method of solution used here is the Runge-Kutta procedure, which in this case may be outlined as follows: (Ref. 64)

The x-dimension is divided into increments Δx for the points x_1, x_2, x_3, ... x_n

Assuming U_i is given at x_i, the derivative

$$\frac{dU_i}{dx_i} = \frac{U_{i+1} - U_{i-1}}{2\Delta x}$$

and $\beta_i = f(\alpha_i, R_{\delta_i})$ (equation (59))

For second order accuracy

$$\delta_{i+1} = \delta_i + \frac{1}{2}(\Delta\delta_1 + \Delta\delta_2)$$

where $\Delta\delta_1 = F_1(\alpha_i, \beta_i, \delta_i, U_i)$

$$\Delta\delta_2 = F_1(\alpha_1 + \Delta\alpha_1,\ \beta_i',\ \delta_i + \Delta\delta_1,\ U_{i+1})$$

$$\beta_i' = f(\alpha_i + \Delta\alpha_1,\ R_{\delta_{i+1}})$$

A similar procedure is followed for α, which gives

$$\alpha_{i+1} = \alpha_i + \frac{1}{2}(\Delta\alpha_1 + \Delta\alpha_2)$$

The process is then repeated for as many values of x as desired or until $\alpha = 0$, where the calculation breaks down.

No general rule can be given for the step size, but for starting values of $H = 1.4$, steps of several boundary layer thicknesses were used with no difficulty. However, for large values of $H > 2.2$, the calculations showed a tendency to ocsillate for large values of $\Delta x/\delta$. Most of the calculations reported here were for approximately 30 - 40 steps.

An estimate of the errors involved can be obtained by doubling the number of steps. The number was doubled in several cases for the present analysis, with almost no change in the result.

The computer program is given in Appendix B.

(f) Comparison of Theory with Experiment

It should be pointed out that the preceding analysis in no way depends on the data with which it will now be compared; no constants are left undetermined. The velocity profiles, of course, were based on a large number of experiments, but not including the present ones. Some of the turbulent measurements of this investigation were used to justify the assumption that the eddy viscosity based on zero pressure gradient was reasonable.

Before comparing the theory with the present experiments, some correction must be made for the fact that the boundary layer was axisymmetric and not two-dimensional in the usual sense. Since the boundary layer

was fairly thin compared to the radius of the cylinder ($\delta/r \leq .3$) this effect might be neglected as a first approximation. However, with the assumptions already made, the equations can easily be transformed for this case (Appendix C).

Figure 18 shows the comparison of the approximate theory with experiment for the linear pressure distribution (2). The experimental pressure distribution is shown again in Figure 18a along with the experimental and calculated values of Θ, both as a function of x. Figure 18b shows the corresponding values of H and α. The experimental values of α were determined from the velocity profiles, which were plotted on logarithmic charts. The profiles are shown in Figure 18c, both experimental and calculated values. As can be seen, the agreement between theory and experiment is very good, especially for the parameters Θ, H and α.

Figure 19 shows the comparison of theory and experiment for the three different pressure distributions. The agreement is not quite as good in the two new cases as with the linear pressure distribution, but still reasonably good for an approximate theory.

(g) Reliability

Since there are no exact solutions for turbulent flow, the approximate theories can only be checked by experimental means. In this case there are two sources of errors, those involved in the approximations and the experimental ones. These errors may often compensate for each other, especially if the approximate methods are based on the experiments. Although the present method agrees very well with the experiments, a reasonable amount of uncertainty must be admitted.

Again the main source of errors in the approximations is the turbulent shear stress, but it is difficult to determine just how much uncertainty is involved. In order to determine the sensitivity of the final

result to errors in the eddy viscosity, equation (66), values of ± 15 percent were assumed. In some cases these values are probably exceeded, but the average should be within this range, since most calculations start from zero pressure gradient. The resulting errors in the calculation of the shape factor and momentum thickness are shown in Figure 20, for the linear pressure gradient.

In order to obtain a more general idea of the effect of errors in the eddy viscosity, three general types of pressure distributions were calculated. Since the pressure rise to separation is of primary importance, the calculations were carried to the point where $c_f = 0$. These points were then plotted as a function of x/δ_1. The resulting curves, Figures 21, 22 and 23, show the pressure rise to separation, hypothetically, for the three general types, with the uncertainty due to the assumed range of ± 15 percent in the eddy viscosity.

Experimental errors enter into the calculations through the initial conditions and pressure distribution. If the boundary layer is allowed to develop for some distance in zero or a mild pressure gradient, the initial conditions are not very important. Some idea of this effect can also be gained from Figures 21, 22 and 23 by a change in x/δ_1, which becomes less important at large values.

One of the main difficulties in comparing the theory with experiment is the pressure distribution near separation. In this region the pressure depends on the behavior of the boundary layer, which in turn is very sensitive to the pressure. By assuming the pressure independent of the boundary layer, one would be very fortunate to calculate a flow that would give this pressure. These facts are illustrated by assuming a slight change in the linear pressure distribution, Figure 24.

V. SUMMARY and CONCLUSIONS

In attempting to predict the behavior of turbulent boundary layers, it is safe to conclude that some assumption must be made for the velocity profiles.

$$\frac{u}{U} = f(\eta, \alpha, \beta, \ldots .)$$

With the present uncertainty in the turbulent shear stress, it is unlikely that anything can be gained by leaving more than one of the parameters, $\alpha, \beta, \ldots$, completely free, i.e. to be determined from the momentum equation. It is generally agreed that the assumption for the velocity profiles, within reason, is relatively unimportant. However, if a choice must be made, the most successful correlation so far proposed is the "wall law" with an outer wake region.

In order to determine the boundary layer thickness and the profile parameter, or shape factor, two equations are needed.

$$\frac{d\delta}{dx} = F_1(\alpha, \delta, U)$$

$$\frac{d\alpha}{dx} = F_2(\alpha, \delta, U)$$

There is no definite criterion for the derivation of these equations, but experience has shown that they should involve integrated quantities. Perhaps the most reasonable choice is the usual momentum integral equation and either its first moment or a momentum integral for the inner part of the boundary layer.

Before the momentum integral equations can be used to calculate α and δ, however, some assumption must be made for the Reynolds stresses. The normal stress is a relatively small term and is usually neglected, but several investigators have questioned the validity of this assumption. The inclusion of experimental values of normal stress does have a slight effect on the calculation of the momentum thickness, which is fairly

insensitive to the shear stress within the boundary layer. However, in the calculation of the shape factor, the effect of the normal stress is much smaller than the effect of the uncertainty in shear stress.

The conclusion by several authors that turbulent shear stress within the boundary layer is the most critical part of the approximate methods was substantiated quantitatively in the present analysis. Since the experimental data is both limited and scattered, it seems reasonable to use what has been learned from zero pressure gradient experiments, i.e. assume the eddy viscosity depends only on local Reynolds number. Just how much uncertainty is involved in this assumption is difficult to determine, but for the purpose of investigating the effect on the final result, a range of $\pm$ 15 percent seems reasonable. In calculating the shape factor, the effect of this uncertainty is considerable. However, in calculating the pressure rise to $c_f = 0$, it amounts to only about $\pm$ 5 percent, unless there is an extremely small pressure gradient near the 'separation' point.

It must be concluded that, with the present uncertainty in the turbulent shear stress, any method of predicting the behavior of the boundary layer becomes very approximate as separation is approached. Since the flow of momentum is proportional to velocity squared, the shape of the velocity profile is very sensitive to errors in the pressure and shear stress in this region. However, if the pressure gradient is reasonably large, it is safe to assume that separation will occur with very little further pressure rise.

It is finally concluded that one of the main difficulties with the approximate methods is the attempt to use them under conditions verging on separation, without considering the effect of the boundary layer growth on the pressure. In most cases involving separation, an experimental

pressure distribution is used. Then with any error at all, the boundary layer displacement that is calculated would not result in this pressure. In order to take this effect into account, however, the geometry of the overall flow must be considered.

IV. RECOMMENDATIONS for FURTHER STUDY

Since the prediction of turbulent boundary layer behavior must ultimately rely on empirical results, more reliable experiments will always be useful. In the general case, a more reliable correlation and perhaps a better understanding of the turbulent shear stress is definitely needed.

However, at this time there is probably more to be gained from a complete investigation of separated flow about a particular configuration. In a review of the unsolved problems of fluid mechanics Kline and Dean[45] conclude that the "prediction of the advent and behavior of stall is perhaps the most pressing single problem". An investigation of this type should include both the boundary layer and the separated region.

REFERENCES

1) F. H. Clauser - "Turbulent Boundary Layers in Adverse Pressure Gradients" - Jour. Aero. Sciences, Vol. 21, pp. 91-108 - 1954.

2) S. Goldstein, editor - Modern Developments in Fluid Dynamics - Vols. I and II - Oxford University Press - London - 1938.

3) H. Schlichting - Boundary Layer Theory - McGraw-Hill Book Co. - New York - 1960.

4) B. Thwaites, editor - Incompressible Aerodynamics - Oxford University Press - London - 1960.

5) A. A. Townsend - The Structure of Turbulent Shear Flow - Cambridge University Press - Cambridge - 1956.

6) J. O. Hinze - Turbulence - McGraw-Hill Book Co. - New York - 1959.

7) G. B. Schubauer and C. M. Tchen - Turbulent Flow - Princeton University Press - Princeton - 1961.

8) N. Tetervin and C. C. Lin - "A General Integral Form of the Boundary Layer Equation for Incompressible Flow With an Application to the Calculation of the Separation Point of Turbulent Boundary Layers" - NACA Report 1046 - 1951.

9) C. C. Stewart - "A Comparison of Turbulent Boundary Layer Theories" - Gas Turbine Laboratory Report No. 57 - M. I. T. - 1960.

10) P. S. Granville - "A Method for the Calculation of the Turbulent Boundary Layer" - David Taylor Model Basin Report 752 - 1951.

11) A. Buri - "A Method of Calculation for the Turbulent Boundary Layer with Accelerated and Retarded Basic Flow" - British R. T. P. Trans. 2073 - 1931.

12) A. W. Goldstein and A. Mager - "On Maximum Pressure Rise with Turbulent Boundary Layers" - Jour. Aero. Sciences, Vol. 27, No. 3 - 1960.

13) B. A. Jones - "Method for Prediction of Boundary Layer Separation and Growth for Application to Turbine Blade Design" - ASME Preprint No. 57-F30 - 1957.

14) D. Ross and J. M. Robertson - "An Empirical Method for Calculation of the Growth of a Turbulent Boundary Layer" - Jour. Aero. Sciences, Vol. 21 - 1954.

15) J. M. Robertson - "Prediction of Turbulent Boundary Layer Separation" - Jour. Aero. Sciences, Vol. 24 - 1957.

16) C. T. Hewson - "The Growth and Separation of a Turbulent Boundary Layer" - ASME Symposium on Stall - 1958.

17) A. E. von Doenhoff and N. Tetervin - "Determination of General Relations for the Behavior of Turbulent Boundary Layers" - NACA Report No. 772 - 1943.

18) H. C. Garner - "The Development of Turbulent Boundary Layers" - R. and M. No. 2133 - British ARC - 1944.

19) W. S. Coleman - "Analysis of the Turbulent Boundary Layer for Adverse Pressure Gradients Involving Separation" - Quarterly Appl. Mathematics, Vol. 5, pp. 182-216 - 1947.

20) E. Gruschwitz - "The Process of Separation in the Turbulent Friction Layer" - NACA TM 699 - 1933.

21) B. A. Maskell - "Approximate Calculation of the Turbulent Boundary Layer in Two-Dimensional Incompressible Flow" - British RAE Report Aero. 2443 - 1951.

22) E. Truckenbrodt - "A Method of Quadrature for Calculation of the Laminar and Turbulent Boundary Layer in Case of Plane and Rotationally Symmetric Flow" - NACA TM 1379 - 1955.

23) D. A . Spence - "The Development of Turbulent Boundary Layers" - Jour. Aero. Sciences, Vol. 23 - 1956.

24) H. Schuh - "On Determining Turbulent Boundary Layer Separation in Incompressible and Compressible Flow" - Jour. Aero. Sciences, Vol. 22 - 1955.

25) J. F. Norbury - "An Approximate Method for the Calculation of Turbulent Boundary Layers in Diffusers" - Aero. Quarterly, Vol. 8, p. 58 - 1957.

26) D. A. Ross - "A Physical Approach to Turbulent Boundary Layer Problems" - Trans. ASCE, Vol. 121 - 1956.

27) H. L. Moses - "Boundary Layer Separation - Preliminary Report - Gas Turbine Laboratory Report No. 68 - M. I. T. - 1962.

28) K. F. Rubert and J. Persh - "A Procedure for Calculating the Development of Turbulent Boundary Layers under the Influence of Adverse Pressure Gradients" - NACA TN 2478 - 1951.

29) B. S. Stratford - "The Prediction of Separation of the Turbulent Boundary Layer" - Jour. Fluid Mechanics, Vol. 5, pp. 1-16 - 1959.

30) D. M. Gibson, Jr. and G. L. Mellor - "Incompressible Turbulent Boundary Layers in Adverse Pressure Gradients" - Princeton University - Mech. Engineering Report FLD 5 - 1962.

31) H. B. Squire and A. D. Young - "The Calculation of the Profile Drag on Aerofoils" - R. and M. No. 1838 - British ARC - 1938.

32) V. M. Falkner - "A New Law for Calculating Drag" - Aircraft Engineering 15 - 1943.

33) H. Ludwieg and W . Tillmann - "Investigation of the Wall Shearing Stress in Turbulent Boundary Layers" - NACA TM 1285 - 1950.

34) J. M. Bidwell - "Application of the von Karman Momentum Theorem to Turbulent Boundary Layers" - NACA TN 2571 - 1951.

35) B. G. Newman - "Some Contributions to the Study of the Turbulent Boundary Layer near Separation" - Report ACA-53 - Australian ARC - 1951.

36) D. Ross - "Evaluation of the Momentum Integral Equation for Turbulent Boundary Layers" - Jour. Aero. Sciences, Vol. 20 - 1953.

37) Nguyen Van Le - "The von Karman Integral Method as Applied to a Turbulent Boundary Layer" - Jour. Aero. Sciences, Vol. 19 - 1953.

38) J. F. Norbury - "Some Measurements of Boundary Layer Growth in a Two-Dimensional Diffuser" - Trans. ASME, Jour. Basic Engineering, Vol. 81 - 1959.

39) F. H. Clauser - "The Turbulent Boundary Layer" - Advances in Appl. Mechanics, Vol. 4 - 1956.

40) L. Prandtl - "Motion of Fluids with very Little Viscosity" - NACA TM 452 - 1928.

41) G. B. Schubauer and P. S. Klebanoff - "Investigation of Separation of the Turbulent Boundary Layer" - NACA Report No. 1030 - 1951.

42) K. Fediaevsky - "Turbulent Boundary Layer on an Airfoil" - Jour. Aero. Sciences, Vol. 4 - 1957.

43) P. G. Hill - "Turbulent Wakes in Pressure Gradients" - Gas Turbine Laboratory Report No. 65 - M. I. T. - 1962.

44) S. J. Kline - "On the Nature of Stall" - Trans. ASME, Jour. Basic Engineering, Vol. 81 - 1959.

45) S. J. Kline and R. C. Dean, Jr. - "Unsolved Problems of Fluid Mechanics" - Mech. Engineering, Vol. 80 - 1958.

46) G. B . Schubauer - "Air Flow in the Boundary Layer of an Elliptic Cylinder" - NACA Report 652 - 1939.

47) V. A. Sandborn - "Preliminary Experimental Investigation of Low-Speed Turbulent Boundary Layers in Adverse Pressure Gradients" - NACA TN 3031 - 1953.

48) K. Weighardt and W. Tillmann - "On the Turbulent Skin Friction for Rising Pressure" - NACA TM 1314 - 1951.

49) H. Peters - "On the Separation of Turbulent Boundary Layers" - Jour. Aero. Sciences, Vol. 3, pp. 7-12 - 1935.

50) B. S. Stratford - "An Experimental Flow with Zero Skin Friction" - Jour. Fluid Mechanics, Vol. 5, pp. 17-34 - 1959.

51) D. Coles - "The Law of the Wall in Turbulent Shear Flow" - 50 Jahre Grenszchichtforschung.

52) D. Coles - "The Problem of the Turbulent Boundary Layer" - ZAMP 5 - 1954.

53) D. Coles - "The Law of the Wake in the Turbulent Boundary Layer" - Jour. Fluid Mechanics, Vol. 1, pp. 191-226 - 1956.

54) C. Ferrari - "Wall Turbulence" - NASA RE 2-8-59W - 1959.

55) A. Favre and J. Gaviglio - "Turbulence et Perturbations dans la Couche Limite d'une Plaque Plane" - NATP Report 278 - 1960.

56) J. P. Johnston - "Three-Dimensional Turbulent Boundary Layers" - Gas Turbine Laboratory Report No. 39 - 1957.

57) S. J. Kline and P. Runstadler - "Some Preliminary Results of Visual Studies of the Flow Model of the Wall Layers of Turbulent Boundary Layers" - Trans. ASME, Jour. Appl. Mechanics, Vol. 81 - 1959.

58) A. A. Townsend - "The Properties of Equilibrium Boundary Layers" - Jour. of Fluid Mechanics, Vol. 1 - 1956.

59) D. Coles - "Remarks on the Equilibrium Turbulent Boundary Layer" - Jour. of Aero. Sciences, Vol. 24 - 1957.

60) A. A. Townsend - "The Development of Turbulent Boundary Layers with Negligible Wall Stress" - Jour. of Fluid Mechanics, Vol. 8 - 1960.

61) W. K. Allan - "The Continuously Critical Turbulent Boundary Layer" - Jour. of Fluid Mechanics, Vol. 15 - 1963.

62) A. Pallone - "Non-similar Solutions of the Compressible Laminar Boundary Layer Equation with Application to the Upstream Transpiration Cooling Problem" - Jour. Aero. Sciences, Vol. 28 - 1961.

63) D. Coles - "The Turbulent Boundary Layer in a Compressible Fluid" - Rand Corporation - R-403-PR - 1962.

64) F. B . Hildebrand - Advanced Calculus for Applications - Prentice-Hall - New Jersey - 1963.

APPENDIX A. Derivation of Equations for α, β and δ

The first equation

$$f_1 \frac{d\delta}{dx} + f_2 \frac{d\alpha}{dx} + f_3 \frac{d\beta}{dx} = f_4 \qquad \text{(A-1)}$$

is obtained directly from the velocity profiles, by differentiating equation (59).

The derivation of the two momentum equations is quite straight forward but somewhat tedious, so only the main steps are outlined here. Evaluation of equation (61) at $y = \delta$ and $y = \delta/2$ results in the following:

$$U \frac{\partial}{\partial x}\left[U\delta \int_0^1 \frac{u}{U}\, d\eta\right] - \frac{\partial}{\partial x}\left[U^2\delta \int_0^1 \left(\frac{u}{U}\right)^2 d\eta\right] = \frac{\delta}{\rho}\frac{dp}{dx}$$

$$+ \frac{\tau_w}{\rho} + \delta \int_0^1 \frac{\partial}{\partial x}\left(\overline{u'^2} - \overline{v'^2}\right) d\eta \qquad \text{(A-2)}$$

and

$$(u)_{\eta=.5} \frac{\partial}{\partial x}\left[U\delta \int_0^{.5} \frac{u}{U}\, d\eta\right] - \frac{\partial}{\partial x}\left[U^2\delta \int_0^{.5} \left(\frac{u}{U}\right)^2 d\eta\right] = \frac{\delta}{2\rho}\frac{dp}{dx}$$

$$+ \frac{\tau_w - \tau(.5)}{\rho} + \int_0^{.5} \frac{\partial}{\partial x}\left(\overline{u'^2} - \overline{v'^2}\right) d\eta \qquad \text{(A-3)}$$

which can be written

$$f_5 \frac{d\delta}{dx} + f_6 \frac{d\alpha}{dx} + f_7 \frac{d\beta}{dx} = f_8 \qquad \text{(A-4)}$$

$$f_9 \frac{d\delta}{dx} + f_{10} \frac{d\alpha}{dx} + f_{11} \frac{d\beta}{dx} = f_{12} \qquad \text{(A-5)}$$

where

$$f_5 = \int_0^1 \left[\frac{u}{U} - \left(\frac{u}{U}\right)^2\right] d\eta$$

$$f_6 \frac{d\alpha}{dx} + f_7 \frac{d\beta}{dx} = \delta \frac{d}{dx} \int_0^1 \left[\frac{u}{U} - \left(\frac{u}{U}\right)^2\right] d\eta$$

$$f_8 = \frac{c_f}{2} - \int_0^1 \left[\frac{u}{U} - 2\left(\frac{u}{U}\right)^2 + 1\right] d\eta \cdot \frac{\delta}{U}\frac{dU}{dx}$$

$$+ \frac{\delta}{U^2} \int_0^1 \frac{\partial}{\partial x}\left(\overline{u'^2} - \overline{v'^2}\right) d\eta$$

$$f_9 = \left(\frac{u}{U}\right)_{\eta=.5} \int_0^{.5} \frac{u}{U}\, d\eta - \int_0^{.5} \left(\frac{u}{U}\right)^2 d\eta$$

$$f_{10}\frac{d\alpha}{dx} + f_{11}\frac{d\beta}{dx} = \delta\left(\frac{u}{U}\right)_{\eta=.5}\frac{d}{dx}\int_0^{.5}\frac{u}{U}\,d\eta - \delta\frac{d}{dx}\int_0^{.5}\left(\frac{u}{U}\right)^2 d\eta$$

$$f_{12} = \frac{c_f}{2} - \left(\frac{\tau}{\rho U^2}\right)_{\eta=.5} - \int_0^{.5}\left[\left(\frac{u}{U}\right)_{\eta=.5}\frac{u}{U} - 2\left(\frac{u}{U}\right)^2 + 1\right] d\eta \cdot \frac{\delta}{U}\frac{dU}{dx} + \frac{\delta}{U^2}\int_0^{.5}\frac{\partial}{\partial x}\left(\overline{u'^2} - \overline{v'^2}\right) d\eta$$

Then, with an expression for the velocity profiles in terms of α and β, equation (58), the integrals can be evaluated. However, for small values of η, the logarithmic profiles are negative and should not be used in this region. From Reference 51, equation (58) is valid for $y\,u_\tau/\nu \geq 50$, which results in joining the profiles at a variable η. For the purpose of integration, the velocity is approximated by

$$\frac{u}{U} = k_1\,y + k_2\,(\eta)^{1/5} \qquad 0 \leq \eta \leq 0.1 \tag{A-6}$$

which agrees reasonably well with the empirical results quoted in Reference 51. (A power of 1/7 on the second term was also tried, with similar results.)

The constants k_1 and k_2 may be evaluated by equating the velocity and first derivative of equations (58) and (A-1) at $\eta = 0.1$.

$$\begin{aligned} k_1 &= -2.4816 + 18.2613\,\alpha - 3.1065\,\beta \\ k_2 &= 1.98227 - 6.5467\,\alpha + 2.0338\,\beta \end{aligned} \tag{A-7}$$

Finally, with the above approximations for the velocity profiles, equations (67) and (68) for the normal stress, and $c_f/2 = .16\,\alpha^2$, the functions $f_1 - f_{12}$ can be evaluated.

$$f_1 = \alpha \tag{A-8}$$

$$f_2 = \delta\left[\log\left(\alpha\,R_\delta\right) + 2.1237\right]$$

$$f_3 = -\delta$$

$$f_4 = -\alpha \frac{\delta}{U} \frac{dU}{dx}$$

$$f_5 = .00625 + .88427\,\alpha - .47834\,\beta - 1.45350\,\alpha^2 - .35791\,\beta^2 + 1.39322\,\alpha\,\beta$$

$$f_6 = \delta\,(.88427 - 2.90700\,\alpha + 1.39322\,\beta)$$

$$f_7 = \delta\,(-.47834 + 1.39322\,\alpha - .71582\,\beta)$$

$$f_8 = .16\,\alpha^2 + (-.06568 - 2.0912\,\alpha + 1.44904\,\beta + .9070\,\alpha^2 + .71582\,\beta^2 - 2.78644\,\alpha\,\beta)\,\frac{\delta}{U}\frac{dU}{dx}$$

$$f_9 = .00625 + .38994\,\alpha - .13888\,\beta - .85368\,\alpha^2 - .12914\,\beta^2 + .64466\,\alpha\,\beta$$

$$f_{10} = \delta\,(.73085 - 2.24056\,\alpha + .92132\,\beta)$$

$$f_{11} = \delta\,(-.38479 + 1.02928\,\alpha - .45759\,\beta)$$

$$f_{12} = .16\,\alpha^2 - \left(\frac{\tau}{\rho U^2}\right)_{n=.5} + (-.03568 - 1.69003\,\alpha + .92228\,\beta + 1.57389\,\alpha^2 + .45759\,\beta^2 - 1.95024\,\alpha\,\beta)\,\frac{\delta}{U}\frac{dU}{dx}$$

APPENDIX B. COMPUTER PROGRAM

The computer program for the solution of equations A-1, A-4 and A-5 is shown on the following pages, in Fortran language. It consists of a main program with three subroutines. The input variables with explanations are as follows:

N	Total number of points for which U_i is given (M . MP + 2)
M	Number of printed values (after the initial values)
MP	Number of calculations between printouts
UZERO	Value of U <u>preceding</u> X_1 (necessary for dU at X_1)
DELTAX	Distance between calculation points (ΔX)
AL1	Initial value (α_1)
DEL1	Initial value (δ_1)
X	Initial value (X_1)
U(I)	Values of U_i at X_i (punched six to a card)

The units of length (X, δ) and velocity (U) are arbitrary as long as they are consistent, except in calculating the Reynolds number. In the present calculations units of feet and ft./sec. are used. The Reynolds number for air is then

$$R = \frac{\delta U}{.00016}$$

RUNGE-KUTTA NUMERICAL SOLUTION FOR TURBULENT BOUNDARY LAYERS

```
      DIMENSION U(200)
      READ 10, N, M, MP
10    FORMAT (I6)
      READ 15, UZERO, DELTAX, AL1, DEL1, X
15    FORMAT (F10.5)
      READ 20, (U(I), I = 1, N)
20    FORMAT (6F10.5)
      K = -MP
      PRINT 25
25    FORMAT (56H1TURBULENT BOUNDARY LAYERS IN ADVERSE PRESSURE GRADIENTS,
     1   //4X, 1HX, 11X, 1HU, 8X, 5HALPHA, 7X, 5HDELTA, 8X, 4HBETA, 7X,
     2   5HTHETA, 8X, 1HH//)
      DU = (U(2)-UZERO)/(2.* DELTAX)
      ALPHA = AL1
      DELTA = DEL1
      UE = U(1)
      CALL PRIN(ALPHA, DELTA, UE, X)
      DO 30  J = 1, M
      K = K + MP
      DO 29 JJ = 1, MP
      CALL DER(ALPHA, DELTA, UE, DU, FA, FD)
      AKA = FA * DELTAX
      AKD = FD * DELTAX
      DEL = DELTA + AKD
      AL = ALPHA + AKA
      LL = K + JJ
      UE = U(LL + 1)
      DU = (U(LL + 2) - U(LL))/(2. * DELTAX)
      CALL DER(AL, DEL, UE, DU, FA, FD)
      DELTA = DELTA + .5*(AKD + FD*DELTAX)
      ALPHA = ALPHA + .5*(AKA + FA*DELTAX)
29    X = X + DELTAX
      CALL PRIN(ALPHA, DELTA, UE, X)
30    CONTINUE
      CALL EXIT
      END
```

SUBROUTINE TO COMPUTE DERIVATIVES

```
      SUBROUTINE DER(A, D, U, DU, FA, FD)
      T = LOGF(A*U*D/.00016)
      B = A*(T + 1.1237) - 1.
      F2 = D*(T + 2.1237)
      F4 = -A * D *  DU / U
      F5 = .00625 + .88427*A - .47834*B - 1.4535*A*A - .35791*B*B
     1   + 1.39322*A*B
```

```
      F6 = D * (.88427 - 2.907*A + 1.39322*B)
      F7 = D * (-.47834 + 1.39322*A - .71582*B)
      F8A = .16 * A * A
      F8B = -.06568 - 2.0912*A + 1.44904*B + .907*A*A + .71582*B*B
     1   - 2.78644*A*B
      F8 = F8A + F8B * D * DU/U
      F9 = .00625 + .38994*A - .13888*B - .85368*A*A - .12914*B*B
     1   + .64466*A*B
      F10 = D * (.73085 - 2.24056*A + .92132*B)
      F11 = D * (-.38479 + 1.02928*A - .45759*B)
      F12A = .16*A*A - TAU(U, D, A, B)
      F12B = -.03568 - 1.69003*A + .92228*B + 1.57389*A*A
     1   + .45759*B*B - 1.95024*A*B
      F12 = F12A + F12B * D * DU/U
      G1 = A*F6*F11 + F2*F7*F9 - D*F5*F10 + D*F6*F9 - F2*F5*F11 - A*F7*F10
      G2 = F4*F6*F11 + F2*F7*F12 - D*F8*F10 + D*F6*F12 - F2*F8*F11
     1   - F4*F7*F10
      G3 = A*F8*F11 + F4*F7*F9 - D*F5*F12 + D*F8*F9 - F4*F5*F11 - A*F7*F12
      FD = G2 / G1
      FA = G3 / G1
      RETURN
      END
```

SUBROUTINE TO PRINT VALUES

```
      SUBROUTINE PRIN(A, D, U, X)
      B = A * (LOGF(A*U*D/.00016) + 1.1237) - 1.
      F = .00638 + .8847*A - .4793*B - 1.4527*A*A - .35786*B*B + 1.3927*A*B
      THETA = F * D
      H = (.00833 + .92248 A - .49229 B) / F
      PRINT 1, X, U, A, D, B, THETA, H
    1 FORMAT (F8.4, 4X, F8.3, 4X, 3(F8.5, 4X), F8.6, 4X, F6.3)
      RETURN
      END
```

FUNCTION SUBROUTINE TO COMPUTE TAU

```
      FUNCTION TAU(U, D, A, B)
      TAU = (2.*A - 1.5*B) * (.004/(LOGF(U * D/.00016) - 7.6) + .0013)
      RETURN
      END
```

APPENDIX C. CORRECTION FOR TRANSVERSE CURVATURE

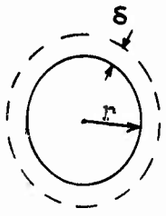

When the boundary layer grows along a body with transverse curvature, such as a cylinder, it is usually assumed that the ratio, δ/r, is small. If this is not true, additional terms appear in the integral equations.

If δ/r is not extremely large it seems reasonable to assume that equation (58) can be used for the velocity profiles. The correction for transverse curvature can then be written

$$f_{ir} = f_i + \frac{\delta}{r} c_i \qquad \text{(C-1)}$$

where f_i are the functions defined in Appendix A.

In the following derivation, the radius is assumed constant, as in the present experiments. The Reynolds' normal stress is neglected, since it already is small and somewhat uncertain.

In this case, the momentum balance can be written

$$u \frac{\partial}{\partial x} \int_0^y u\left(1 + \frac{y}{r}\right) dy + \frac{\partial}{\partial x} \int_0^y u^2\left(1 + \frac{y}{r}\right) dy = \frac{\tau_w}{\rho} - \left(1 + \frac{y}{r}\right)\frac{\tau}{\rho} + \left(1 + \frac{y}{2r}\right) \frac{y}{\rho} \frac{dp}{dx} \qquad \text{(C-2)}$$

Then, with the assumed velocity profiles, the corrections for transverse curvature can be evaluated.

$$f_{5r} = f_5 + \frac{\delta}{r} \cdot 2(.00013 + .24797\,\alpha - .14957\,\beta - .24182\,\alpha^2 - .08547\,\beta^2 + .28170\,\alpha\,\beta)$$

$$f_{6r} = f_6 + \frac{\delta}{r} \cdot \delta(.24797 - .48364\,\alpha + .28170\,\beta)$$

$$f_{7r} = f_7 + \frac{\delta}{r} \cdot \delta(-.14957 + .28170\,\alpha - .17094\,\beta)$$

$$f_{8r} = f_8 + \frac{\delta}{r}(-.00040 - .74462\,\alpha + .44900\,\beta + .48364\,\alpha^2 + .17094\,\beta^2 - .56340\,\alpha\,\beta)\frac{\delta}{U}\frac{dU}{dx}$$

$$f_{9r} = f_9 + \frac{\delta}{r} \cdot 2(.00013 + .06056\,\alpha - .02776\,\beta - .09856\,\alpha^2 - .02276\,\beta^2 + .09227\,\alpha\,\beta)$$

$$f_{10r} = f_{10} + \frac{\delta}{r} \cdot \delta(.14711 - .29958\,\alpha + .15499\beta)$$

$$f_{11r} = f_{11} + \frac{\delta}{r} \cdot \delta(-.09019 + .16619\,\alpha - .09076\,\beta)$$

$$f_{12r} = f_{12} - \frac{\delta}{r}\left(\frac{\tau}{2\rho U^2}\right)_{\eta=.5} + \frac{\delta}{r}(-.00040 - .44204\,\alpha + .27086\,\beta + .40204\,\alpha^2 + .13600\,\beta^2 - .45780\,\alpha\,\beta)\,\frac{\delta}{U}\frac{dU}{dx}$$

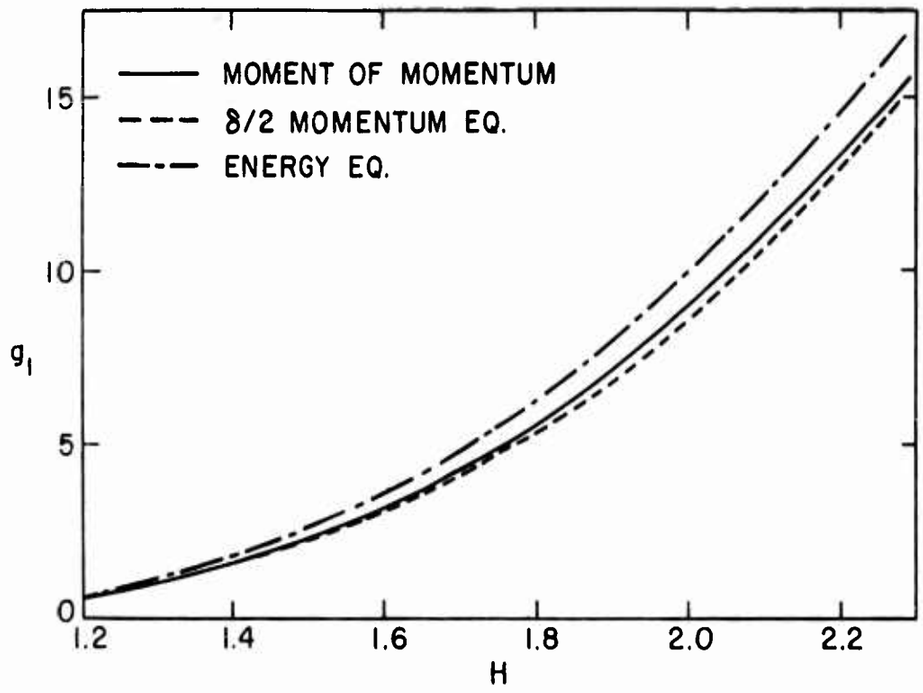

(a) COMPARISON OF DERIVATION FOR POWER LAW PROFILES

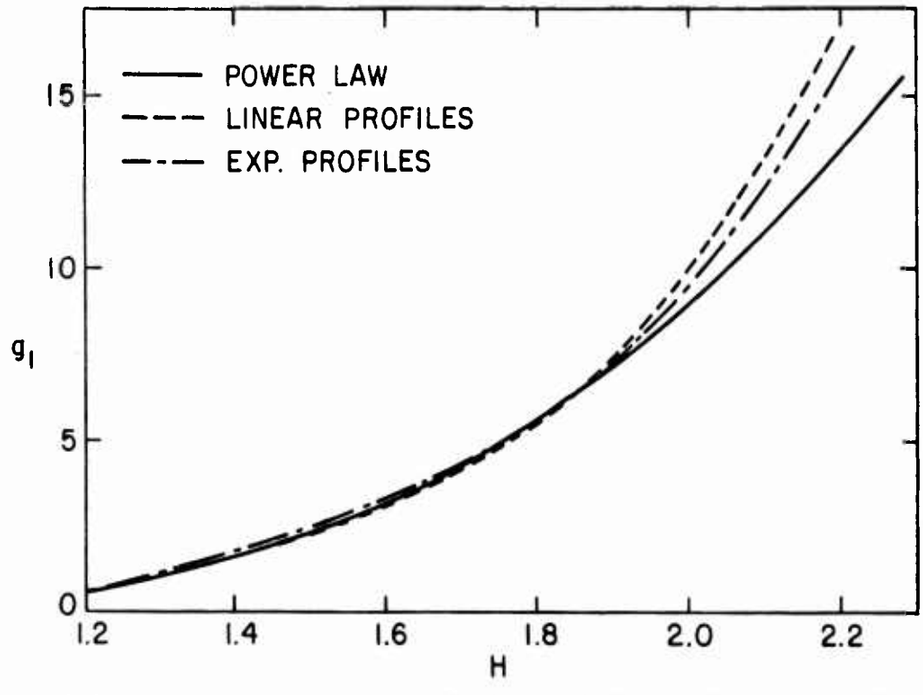

(b) COMPARISON OF VEL. PROFILES FOR MOMENT OF MOMENTUM

FIGURE 1. THE FUNCTION g_1 IN EQUATION (21)

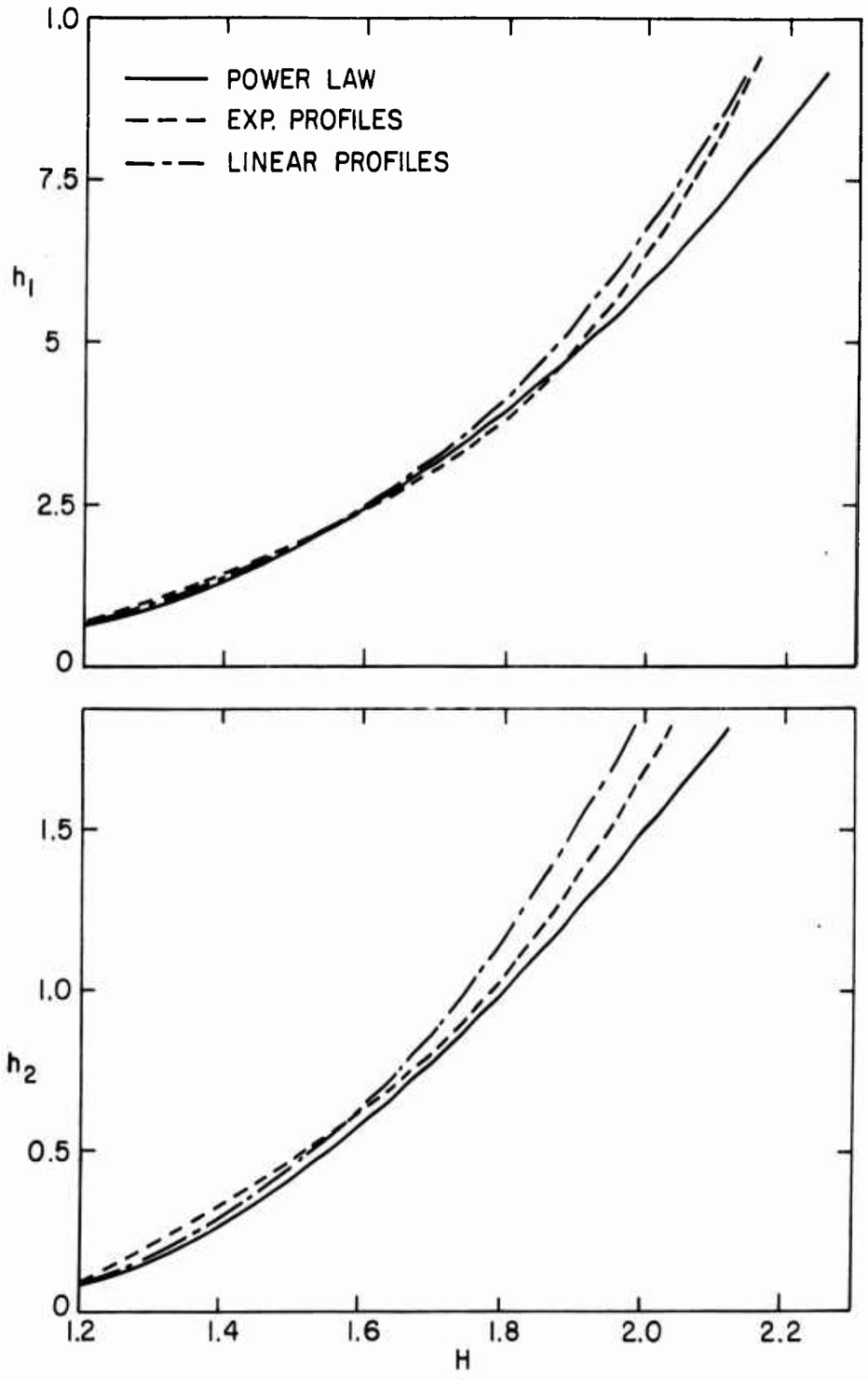

FIGURE 2. THE FUNCTIONS h_1 AND h_2 IN EQUATION (26) FOR THE MOMENT OF MOMENTUM

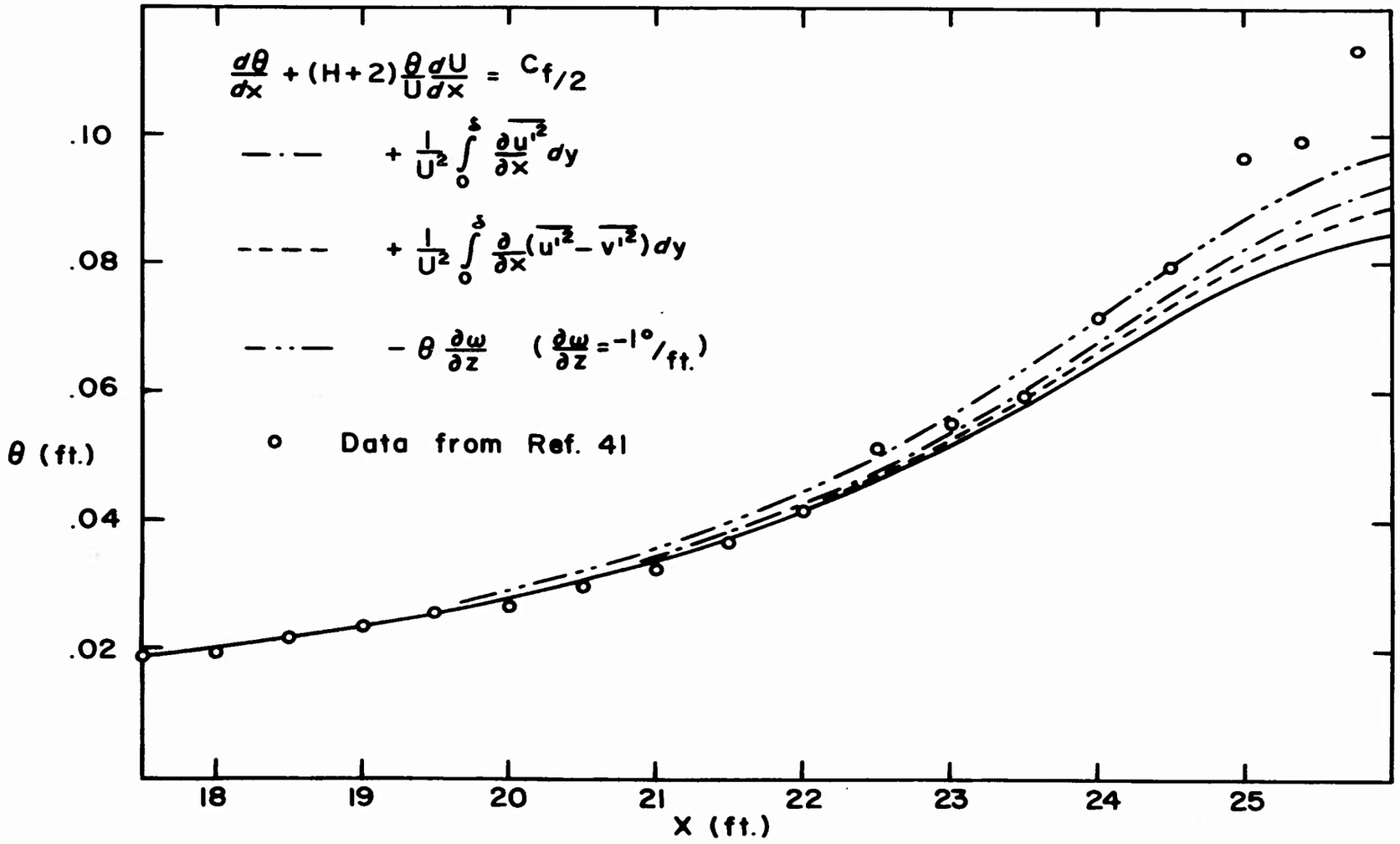

FIGURE 3. MOMENTUM EQUATION

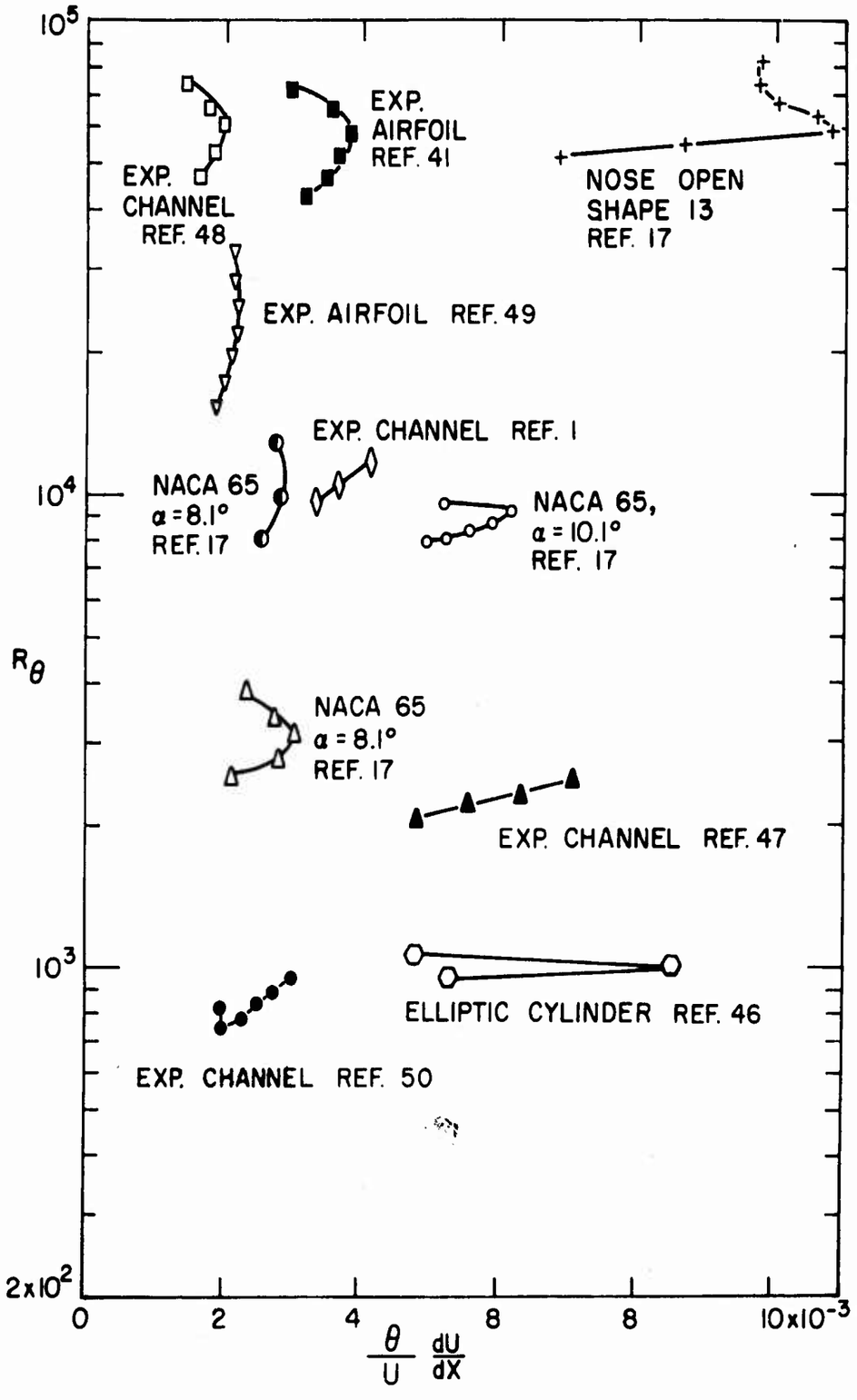

FIGURE 4. CORRELATION OF SEPARATION CRITERIA FOR EXPERIMENTAL DATA NEAR SEPARATION

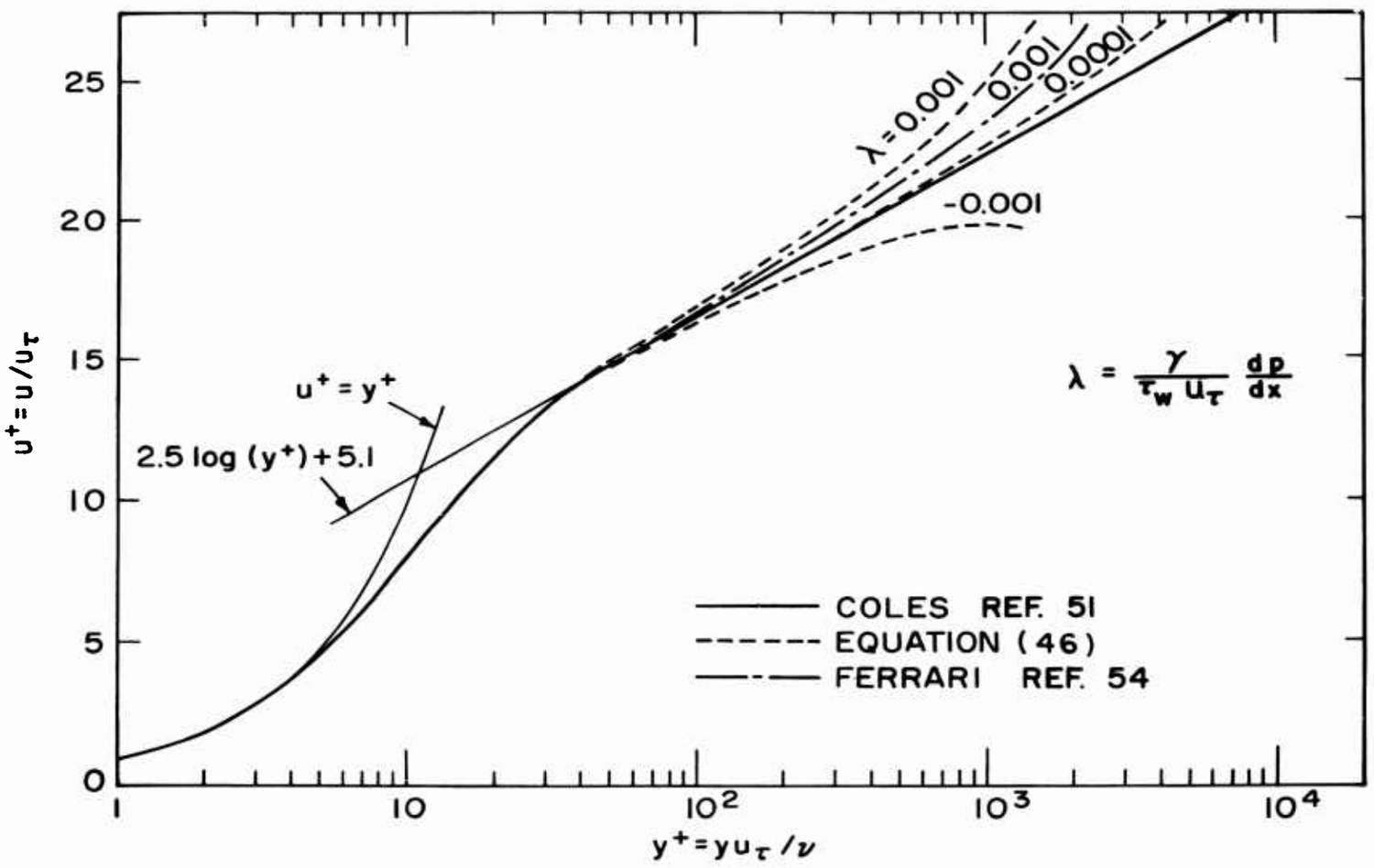

FIGURE 5. LAW OF THE WALL WITH CORRECTIONS FOR PRESSURE

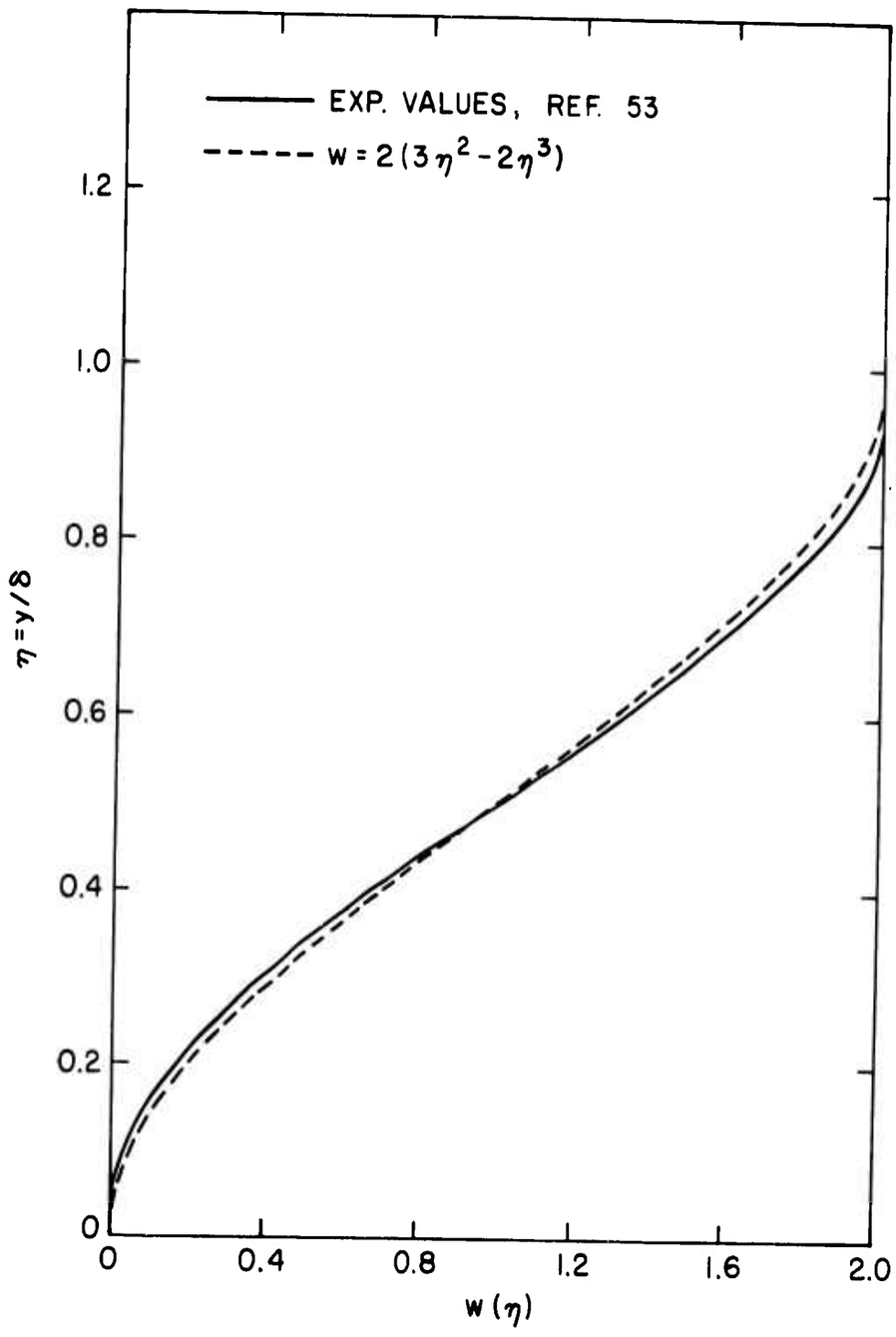

FIGURE 6. UNIVERSAL WAKE FUNCTION

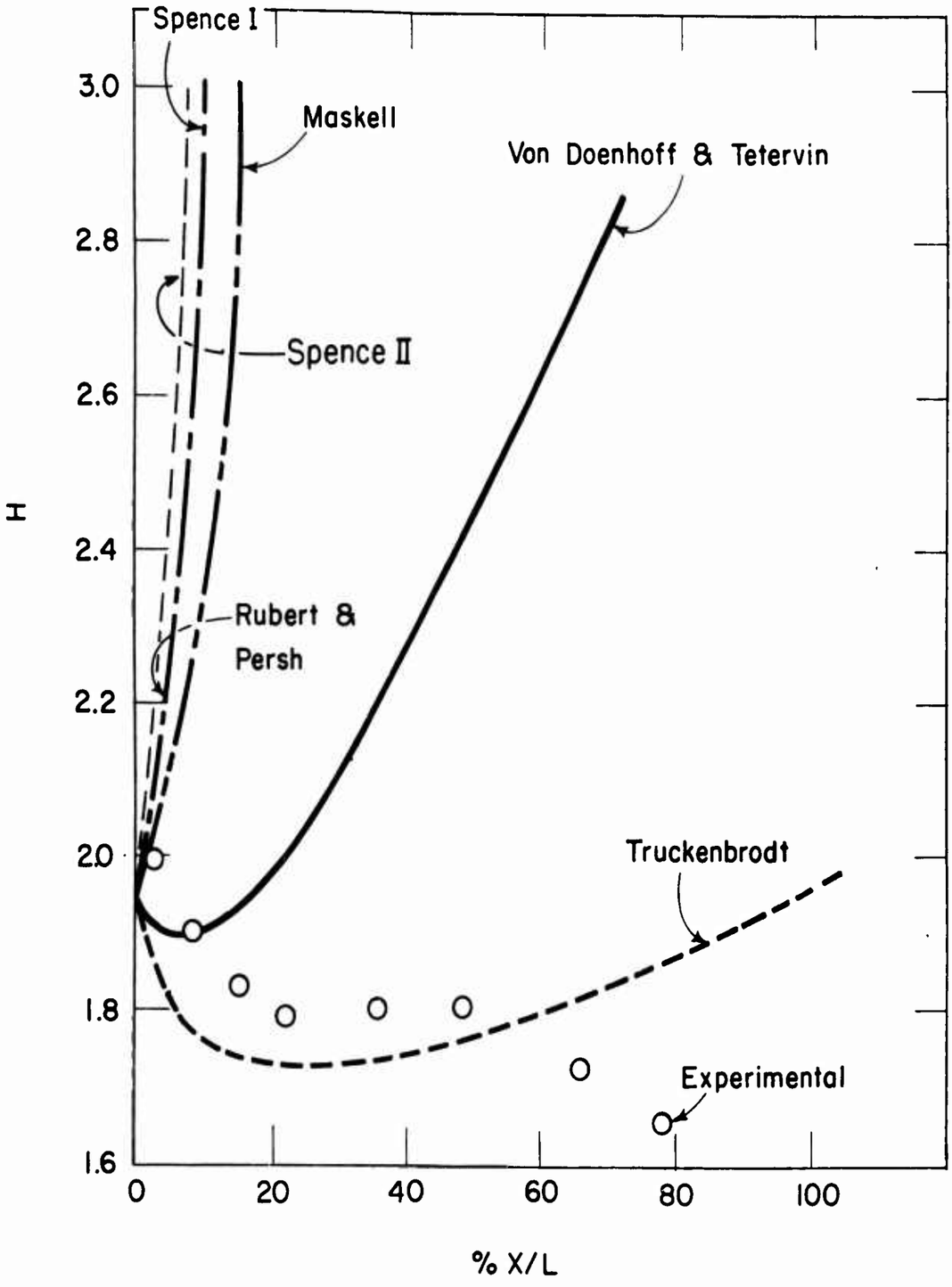

SHAPE FACTOR vs PERCENT OF TEST SECTION LENGTH - CLAUSER'S NO. 2 PRESSURE DISTRIBUTION

FIGURE 7a.

(TAKEN FROM REFERENCE 9)

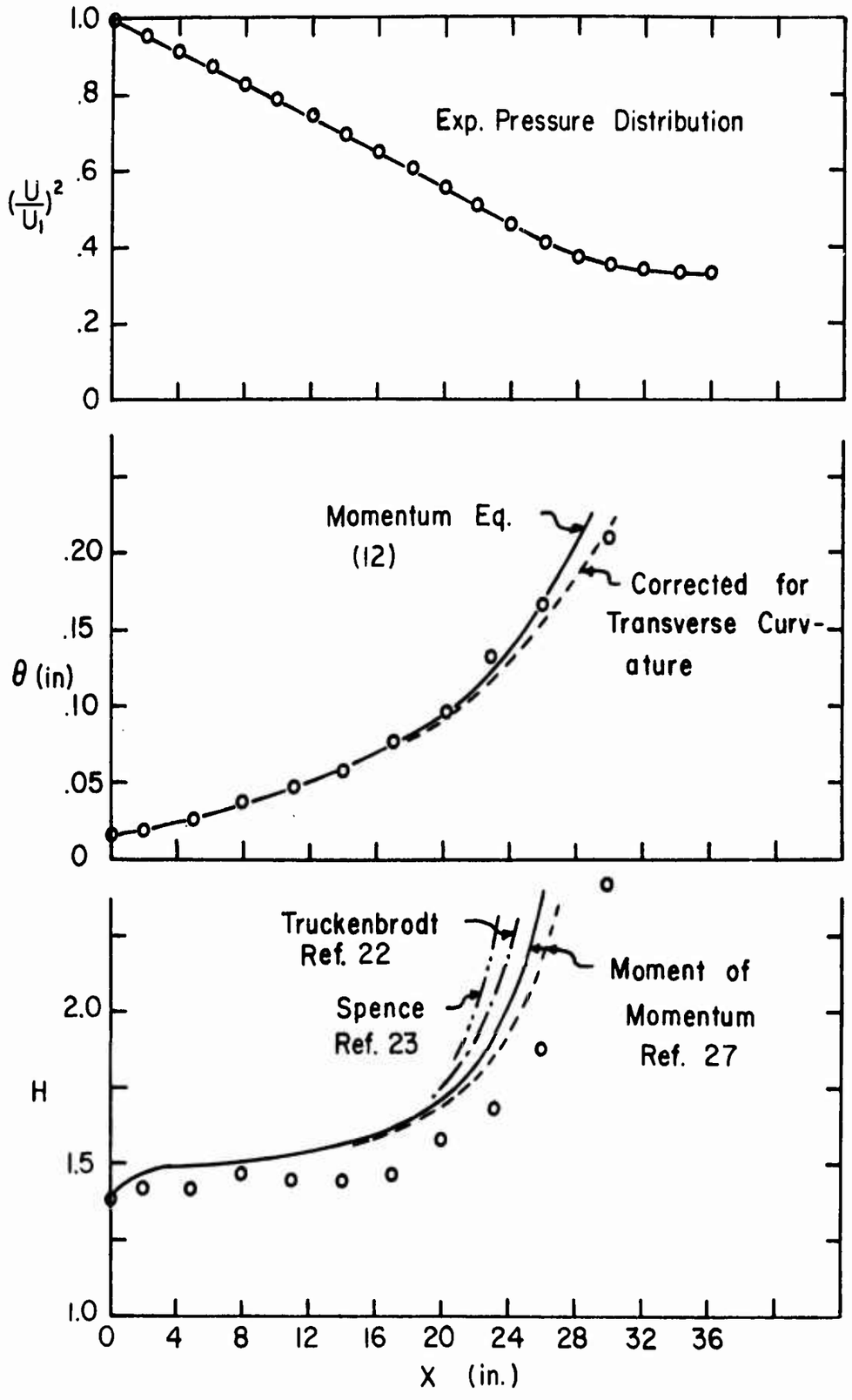

FIGURE 7b. COMPARISON OF EXISTING THEORIES WITH PRESENT EXPERIMENT

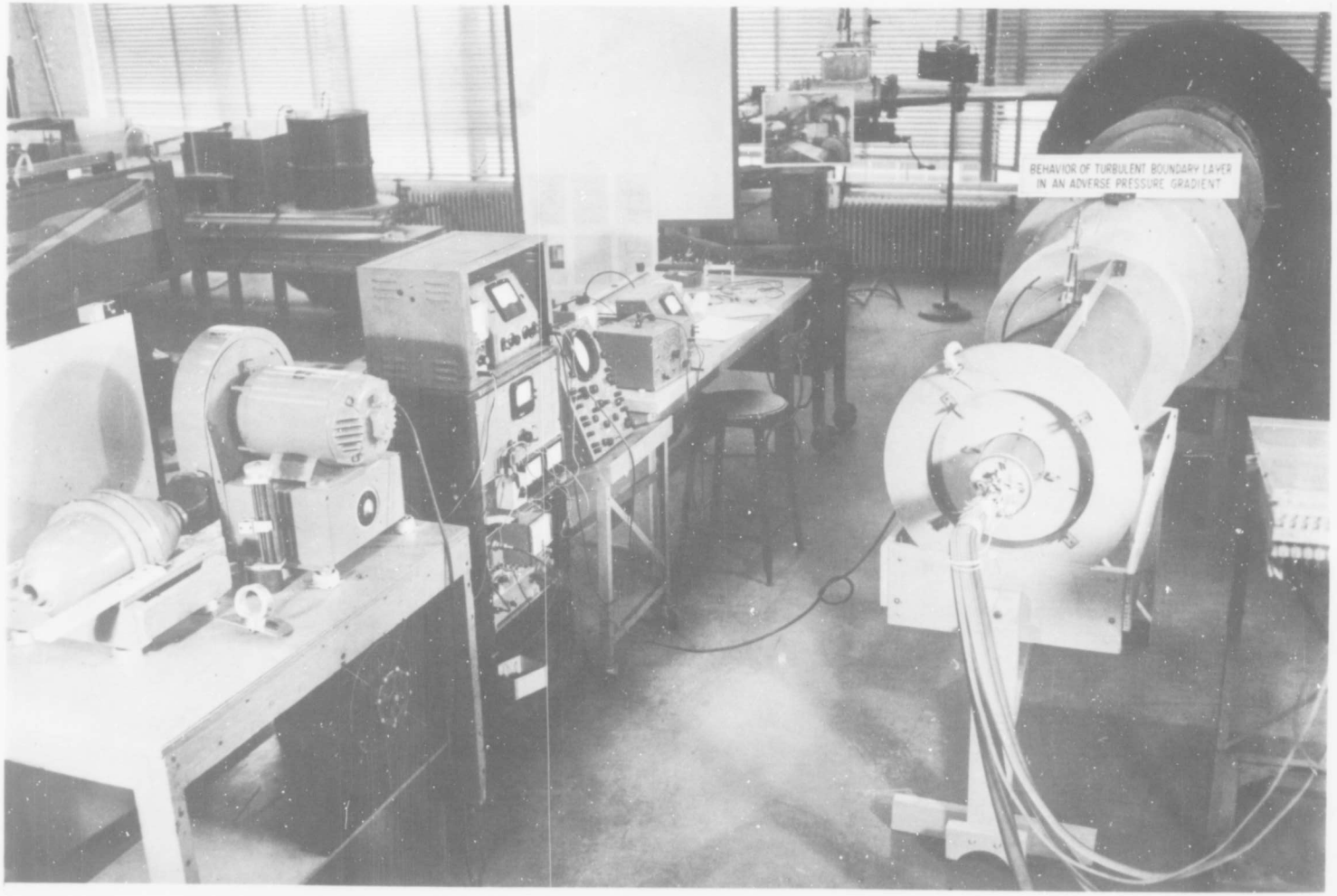

FIGURE 8a. EXPERIMENTAL EQUIPMENT

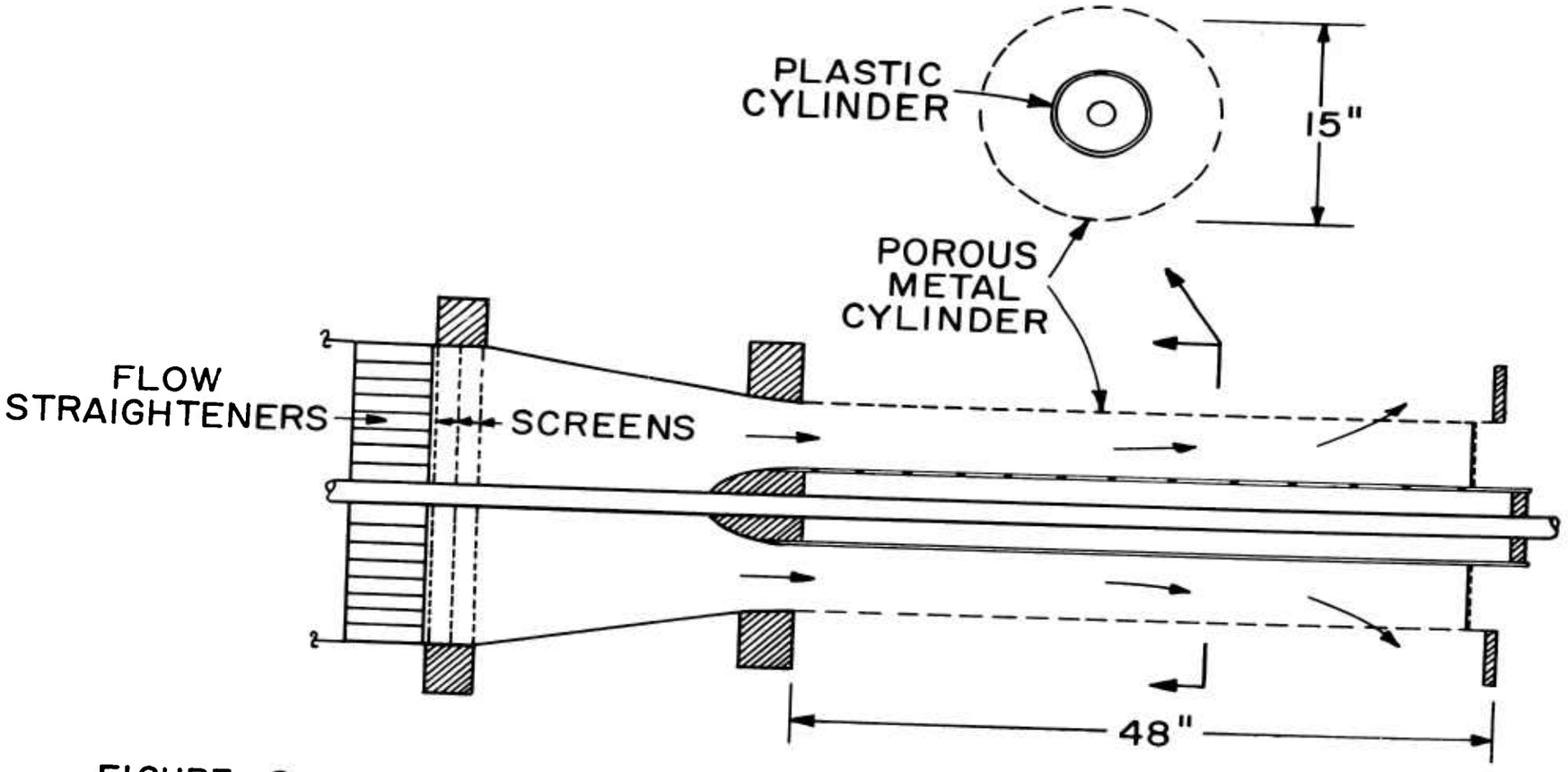

FIGURE 8. b.

TEST SECTION

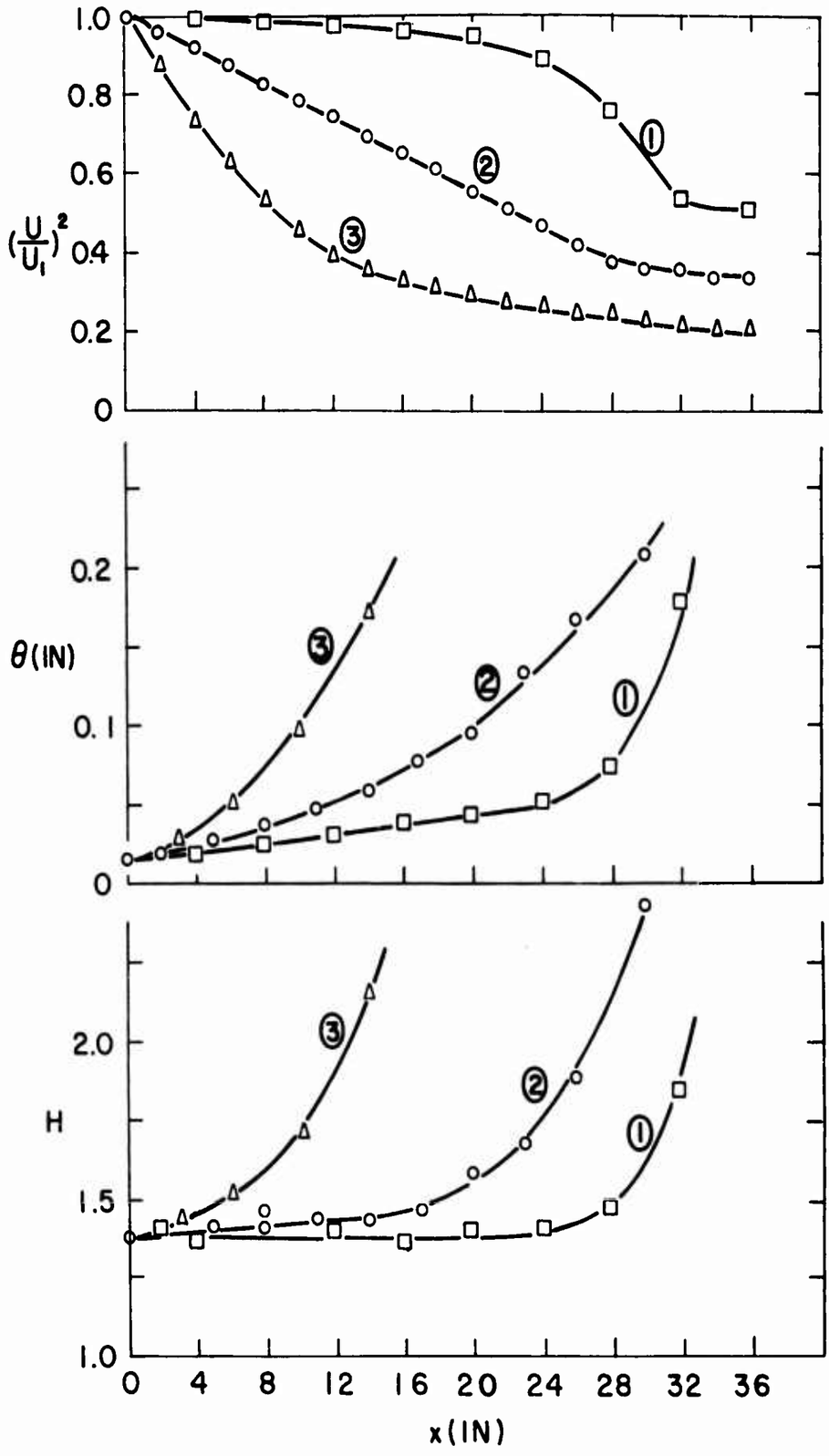

FIGURE 9. EXPERIMENTAL VALUES OF U, θ, AND H

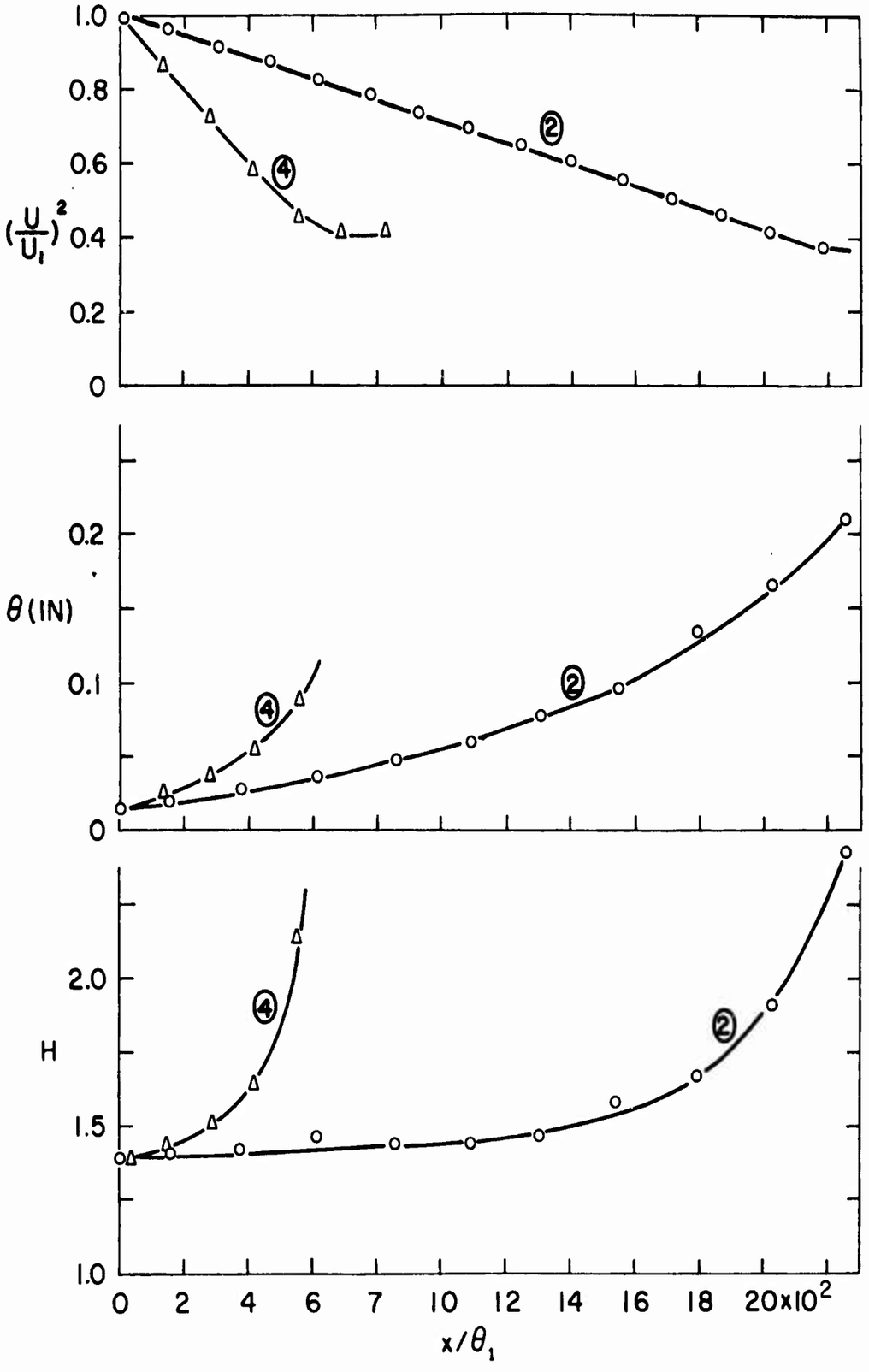

FIGURE 10. EXPERIMENTAL VALUES U, θ, AND H

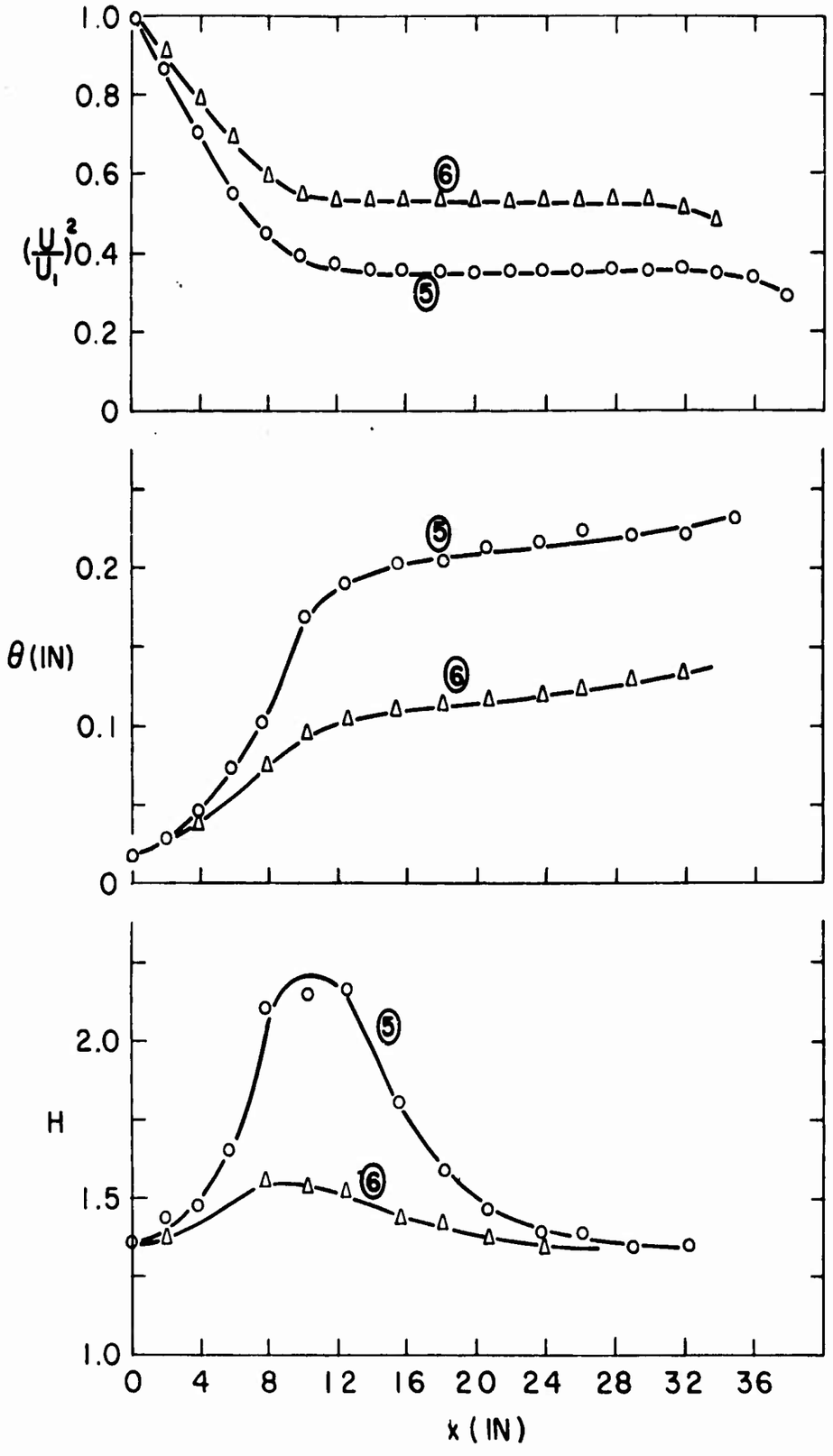

FIGURE II. EXPERIMENTAL VALUES OF U, θ, AND H

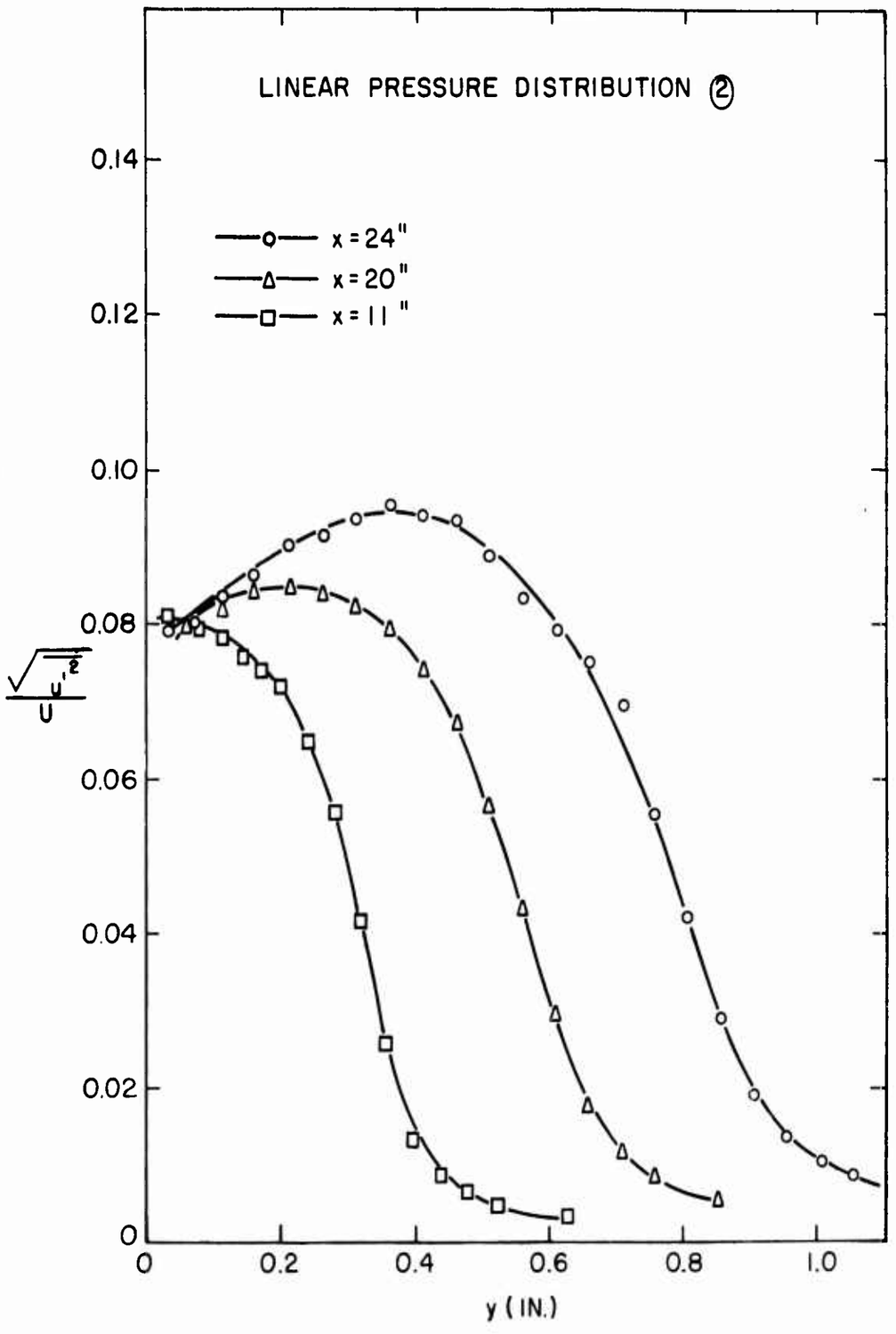

FIGURE 12. TURBULENCE INTENSITY FROM HOT-WIRE MEASUREMENT

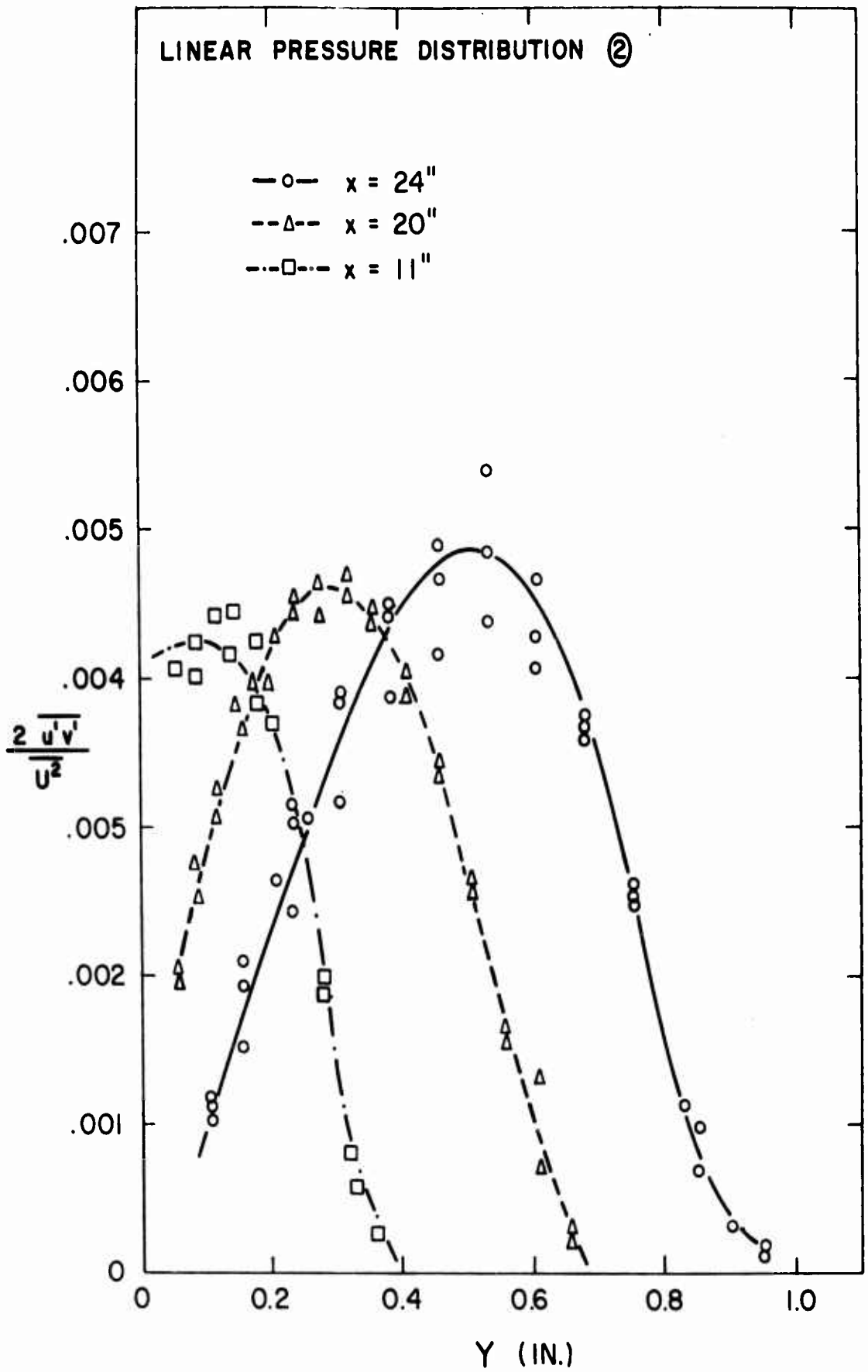

FIGURE 13. TUBULENT SHEAR STRESS FROM HOT-WIRE MEASUREMENT

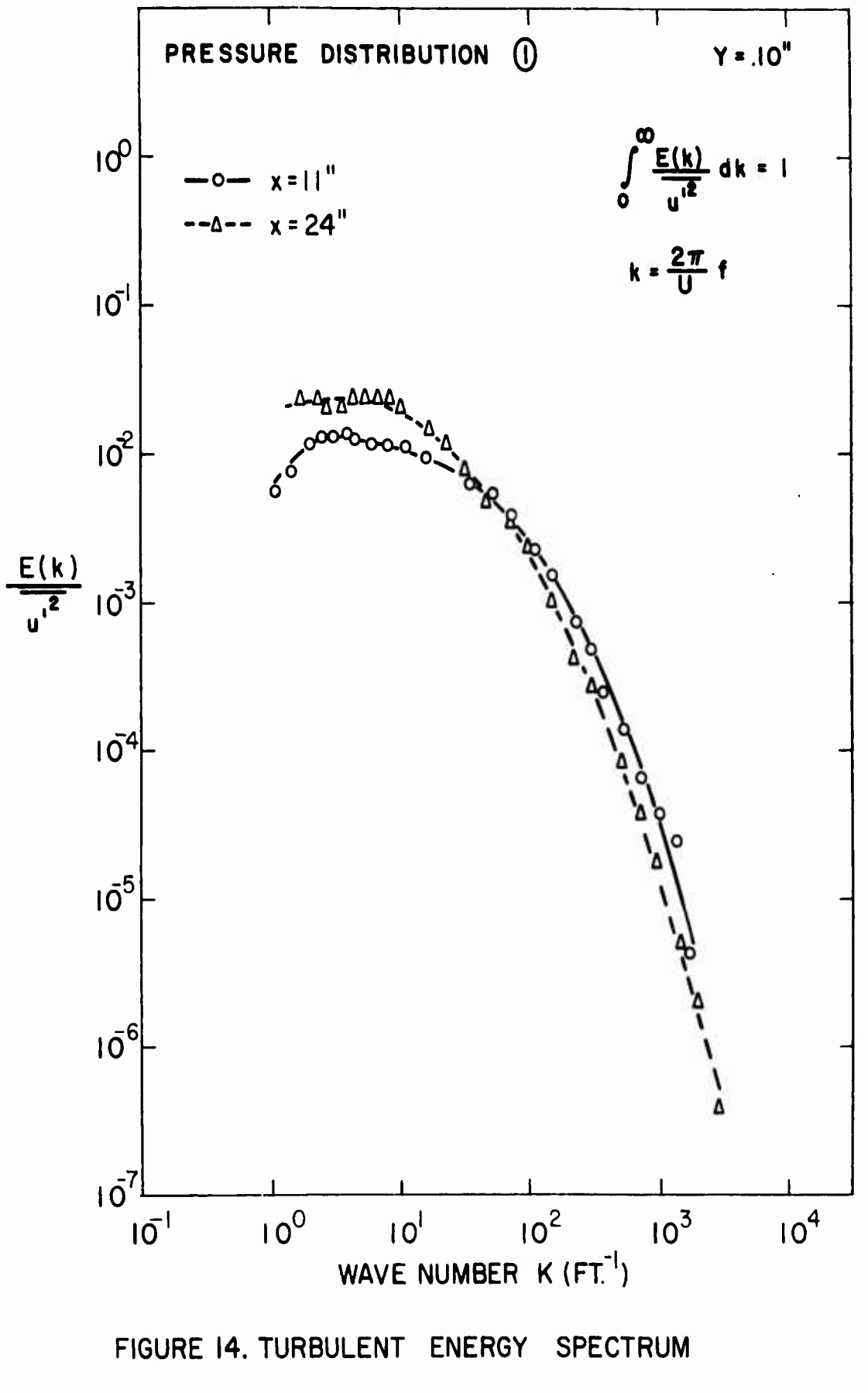

FIGURE 14. TURBULENT ENERGY SPECTRUM

$$\frac{u}{U} = 1 + a \operatorname{Log} \eta + \beta (1 - 3\eta^2 + 2\eta^3)$$

$$\eta = \frac{y}{\delta}$$

$$\beta = a \operatorname{Log} (a R_\delta) + 1.1237\, a - 1$$

$$a = 2.5 \sqrt{C_{f/2}}$$

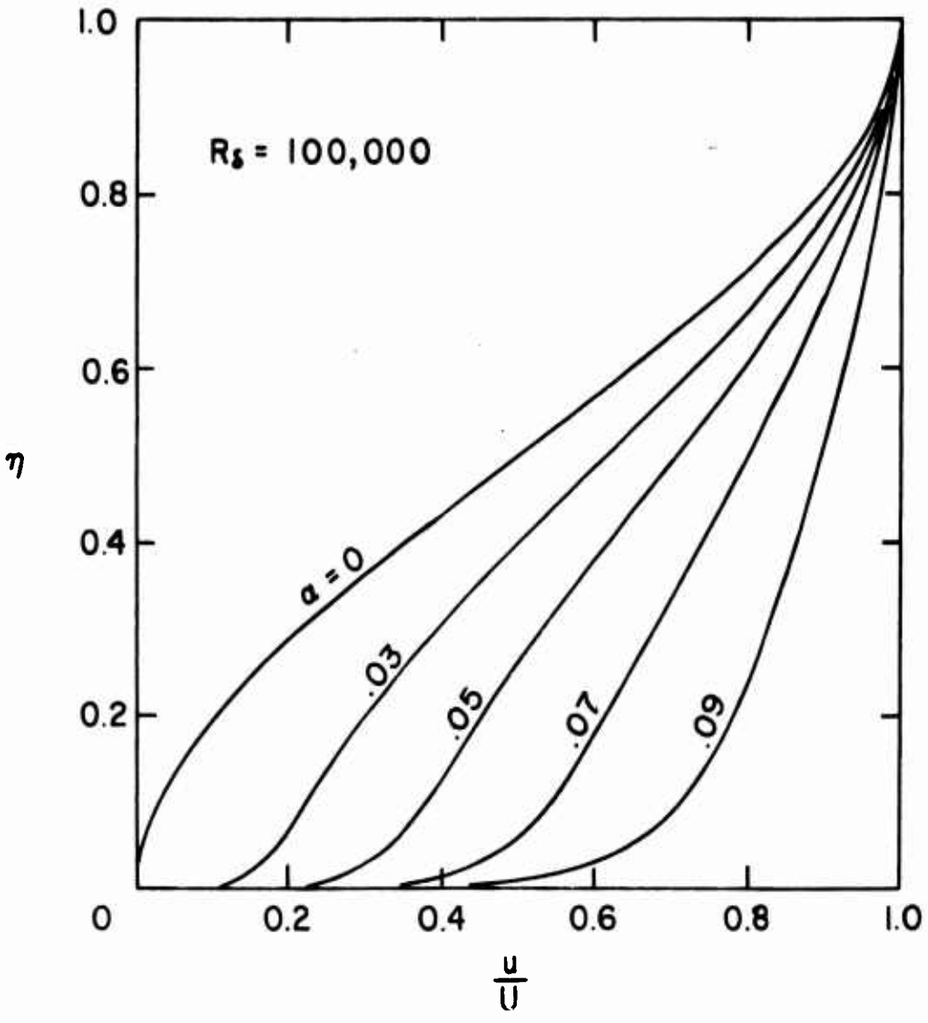

FIGURE 15. TURBULENT VELOCITY PROFILES

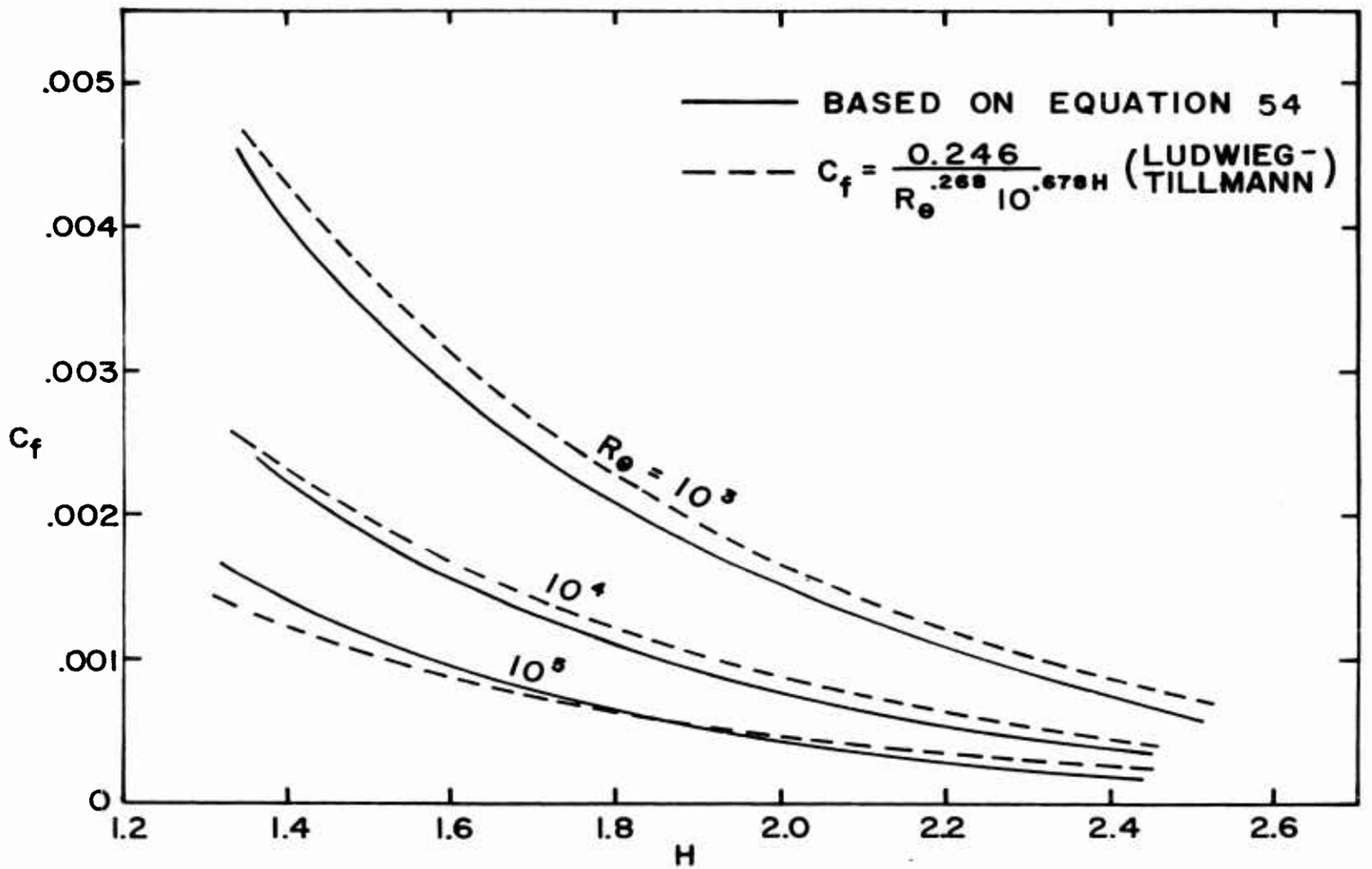

FIGURE 16. TURBULENT SKIN FRICTION

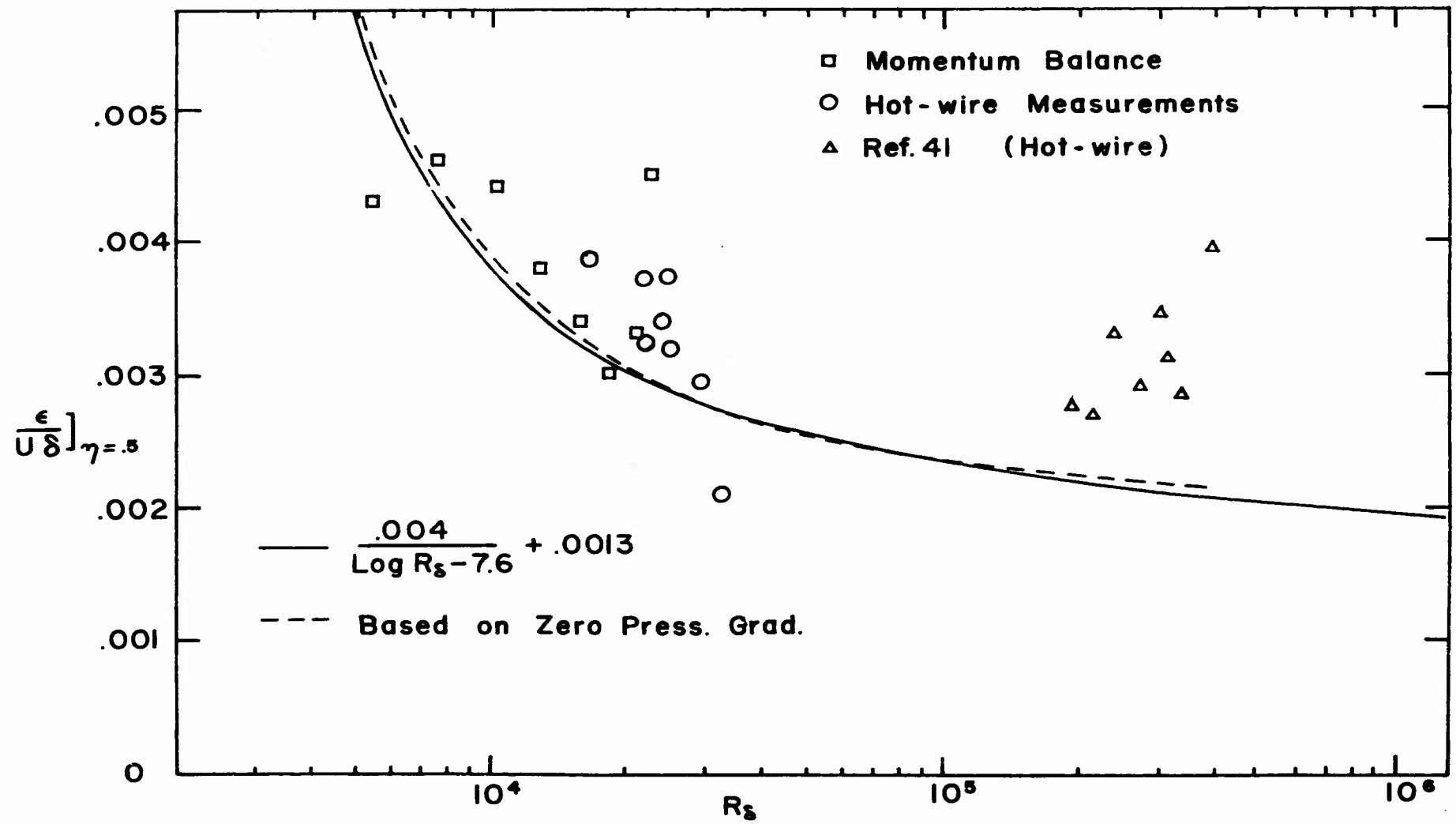

FIGURE 17. EDDY VISCOSITY AT $y/\delta = 0.5$

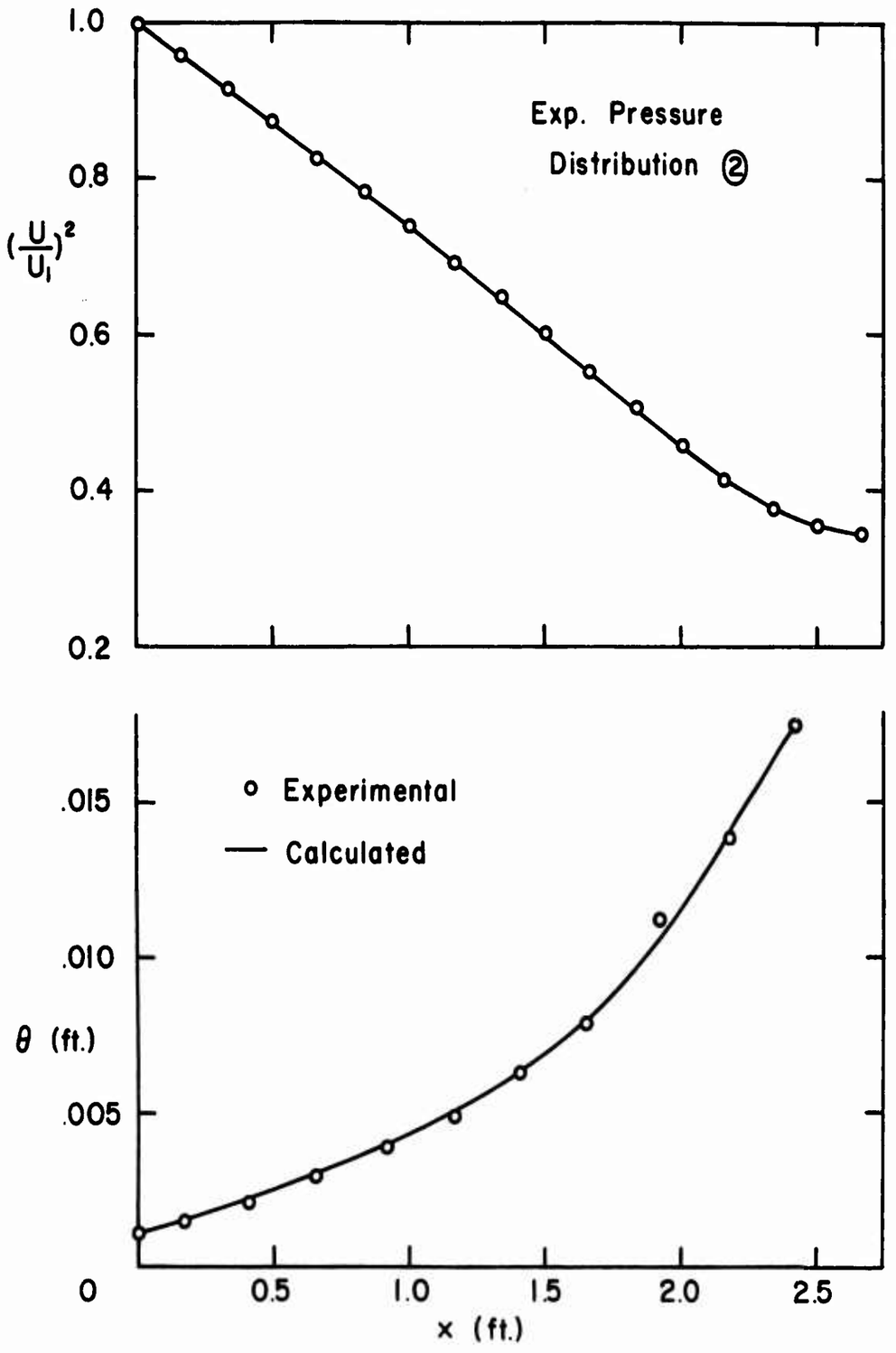

FIGURE 18a. COMPARISON OF THEORY WITH EXPERIMENT

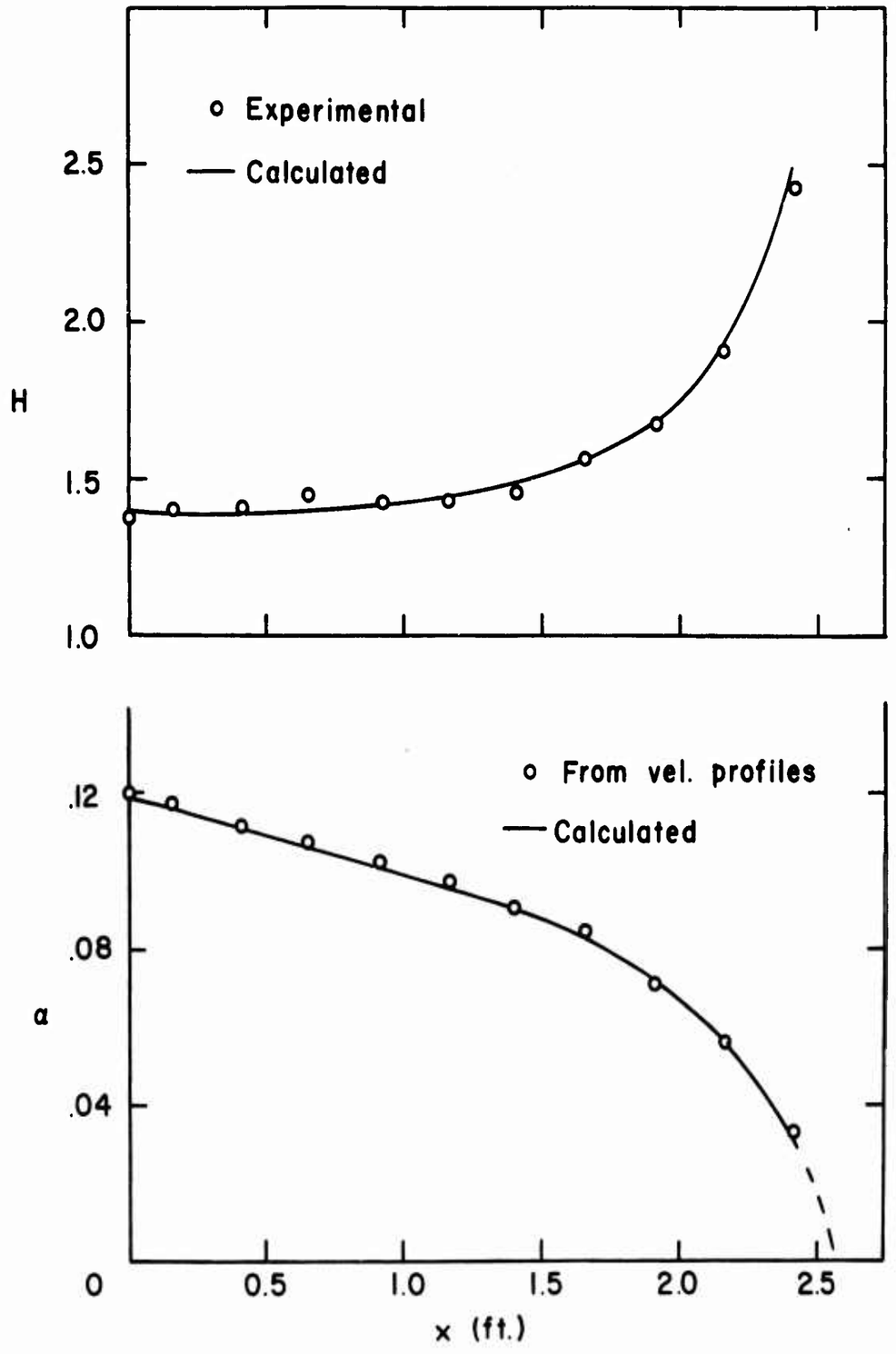

FIGURE 18. (Continued)

b. SHAPE FACTOR & SKIN FRICTION

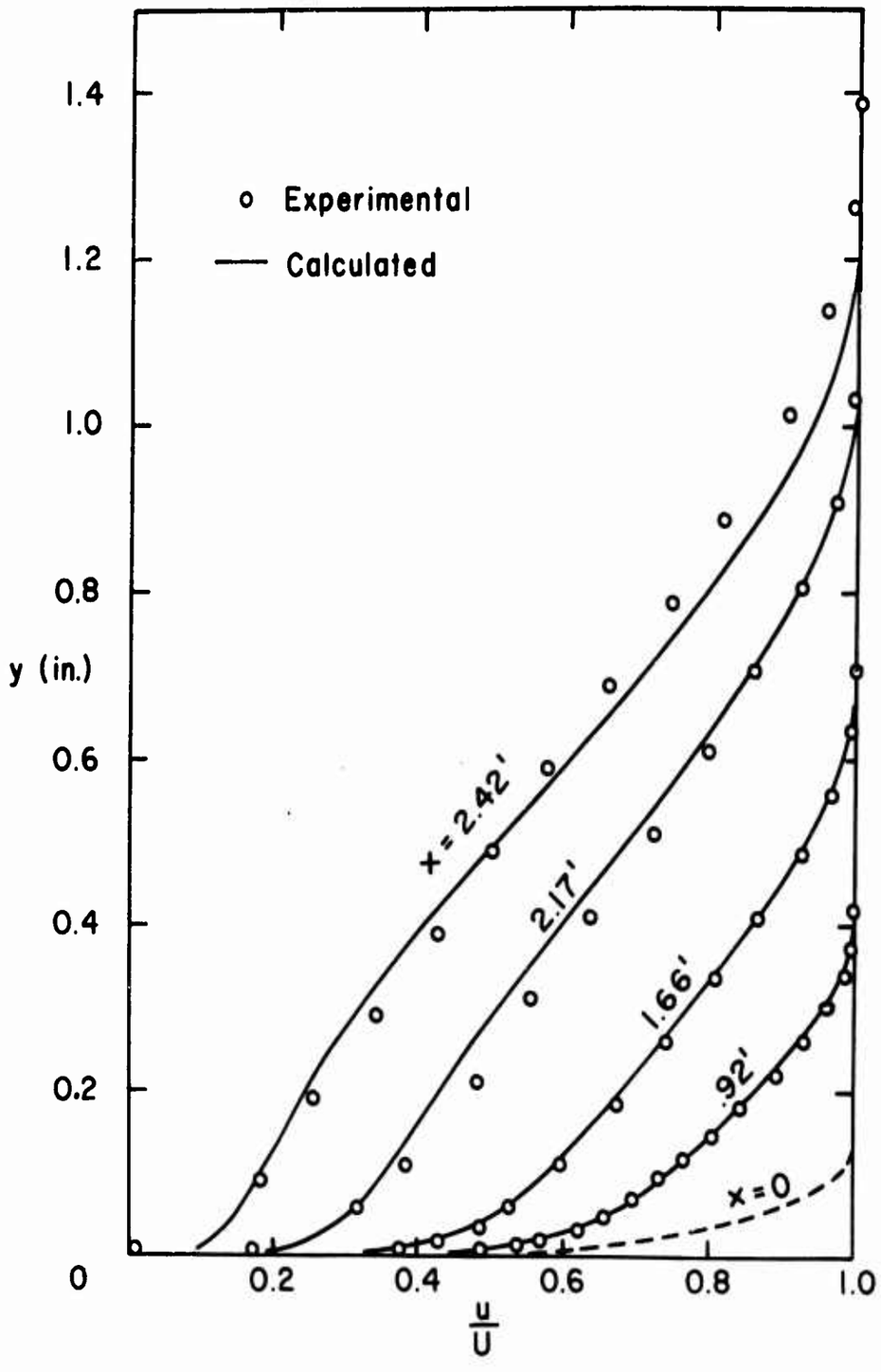

FIGURE 18. (Continued)

c. VELOCITY PROFILES

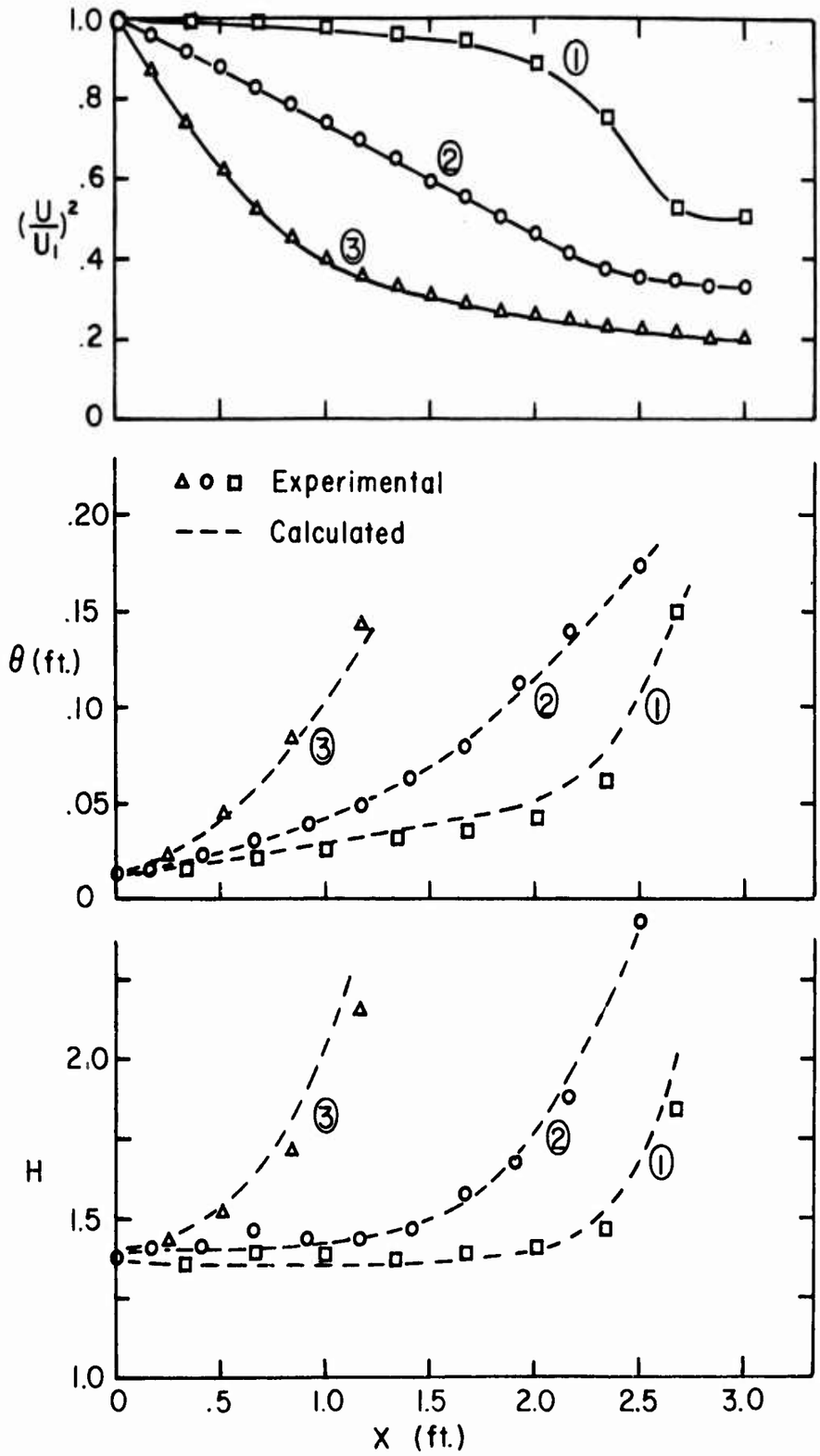

FIGURE 19. COMPARISON OF THEORY WITH EXPERIMENT

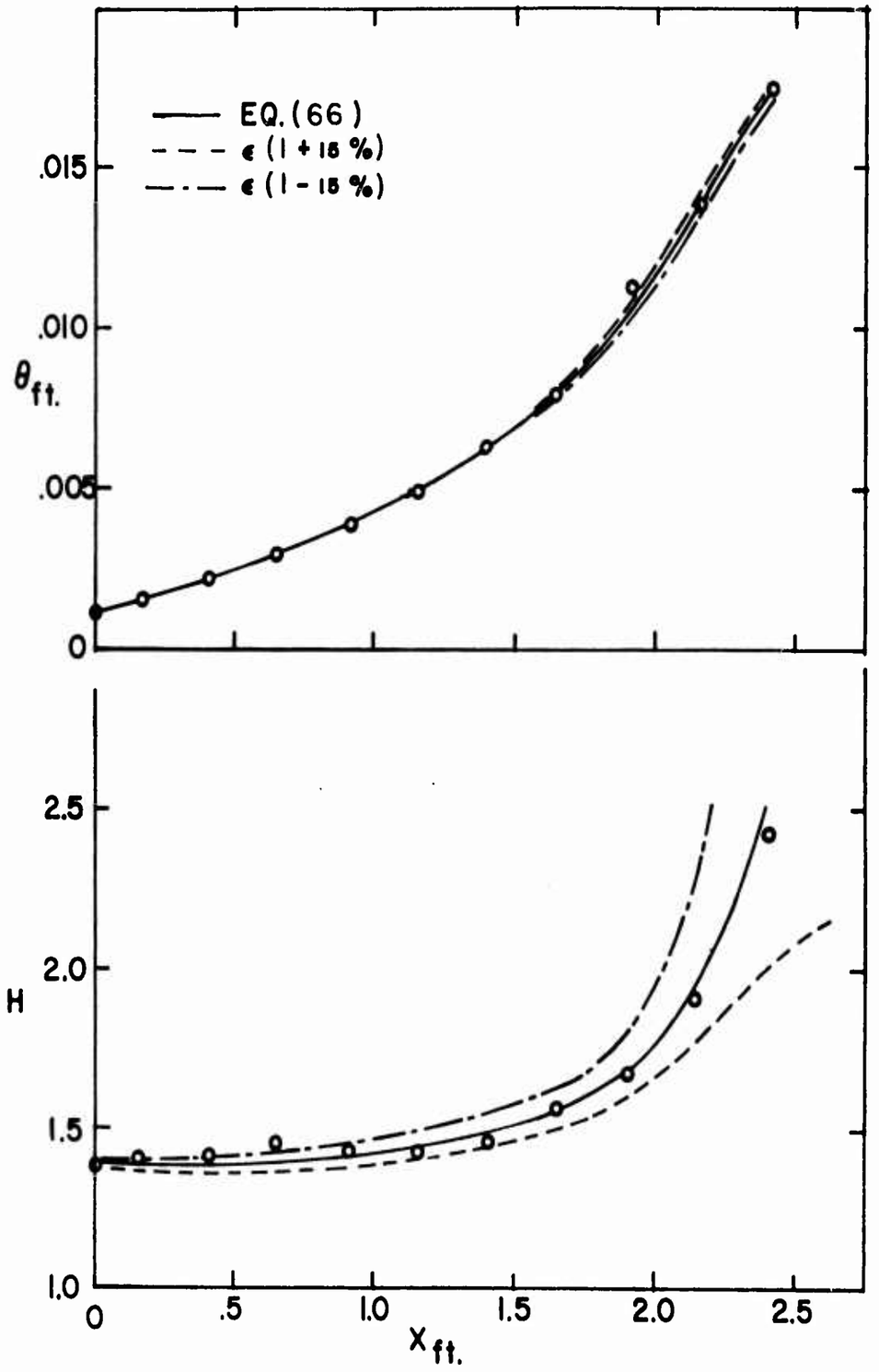

FIGURE 20. EFFECT OF ERROR IN EDDY VISCOSITY FOR PRESSURE DISTRIBUTION (2)

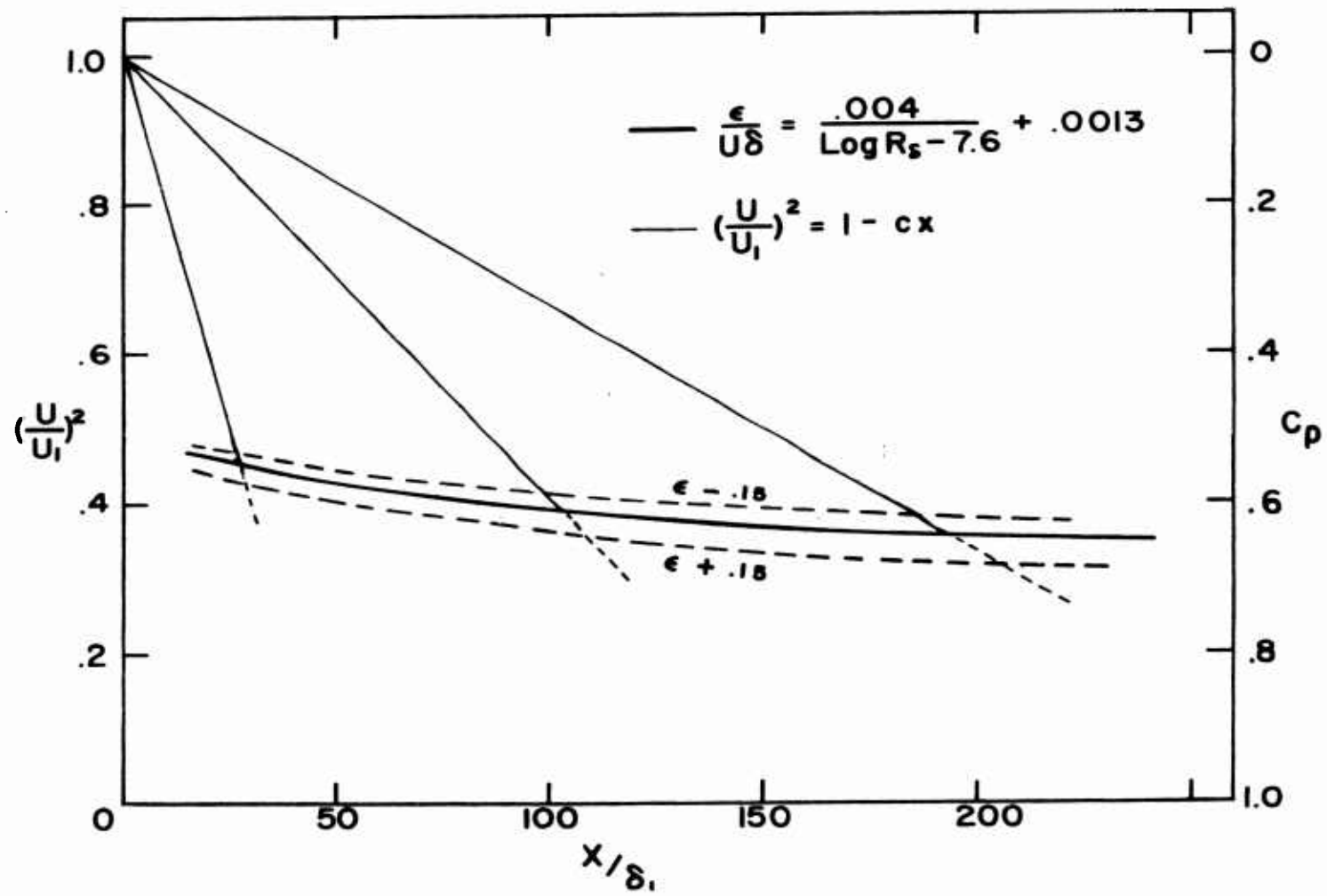

FIGURE 21. PRESSURE RISE TO $C_f = 0$

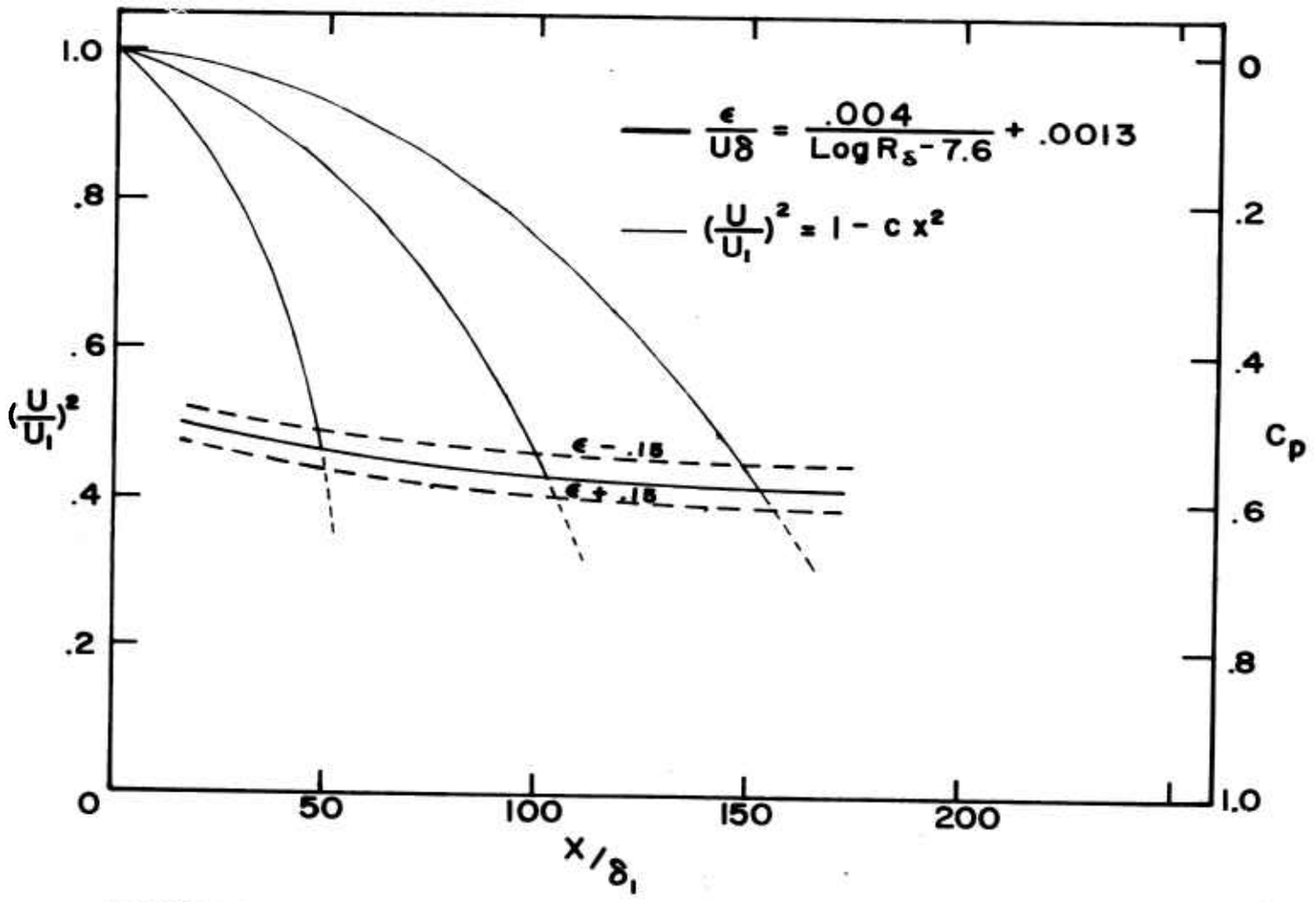

FIGURE 22. PRESSURE RISE TO $C_f = 0$

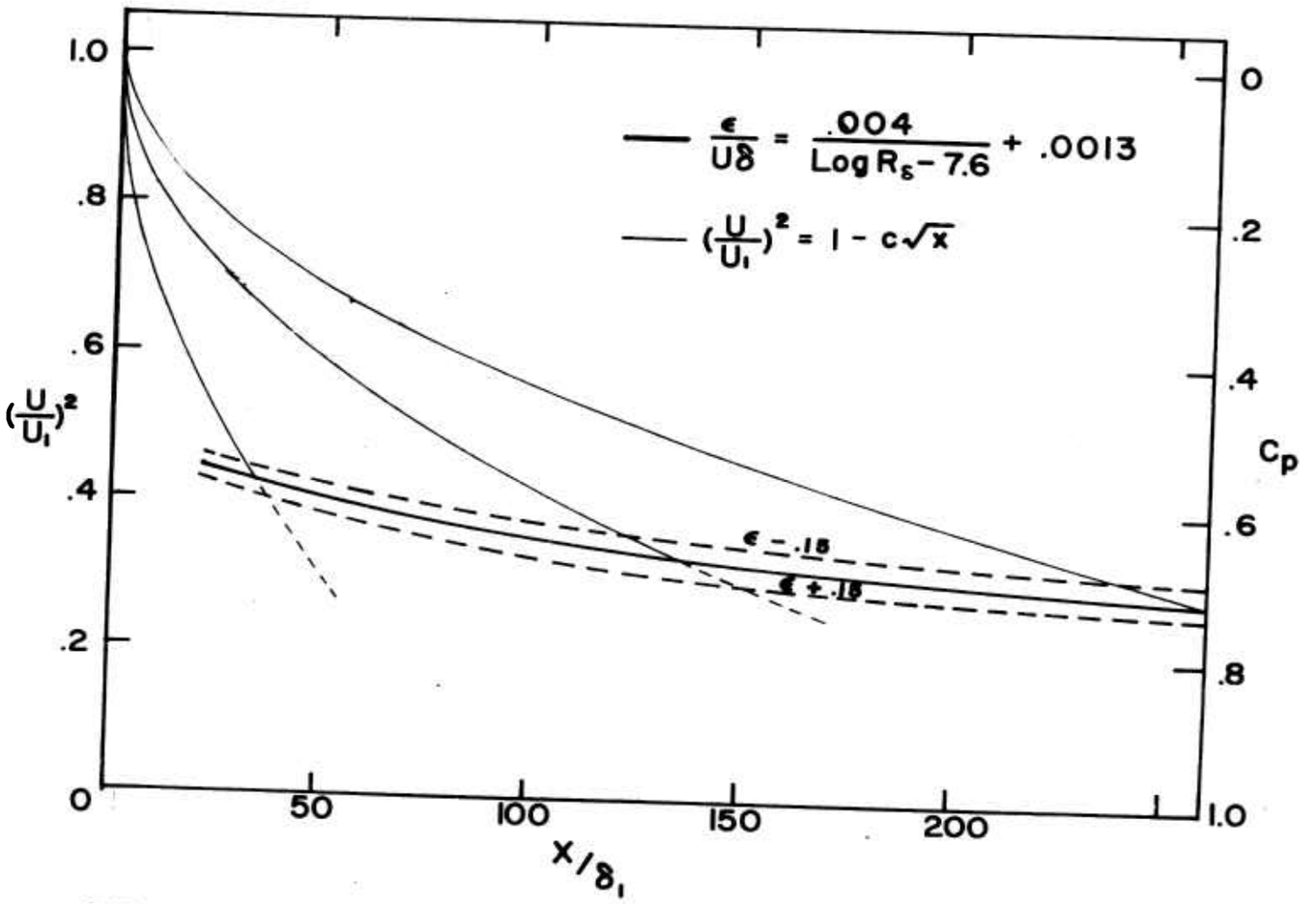

FIGURE 23. PRESSURE RISE TO $C_f = 0$

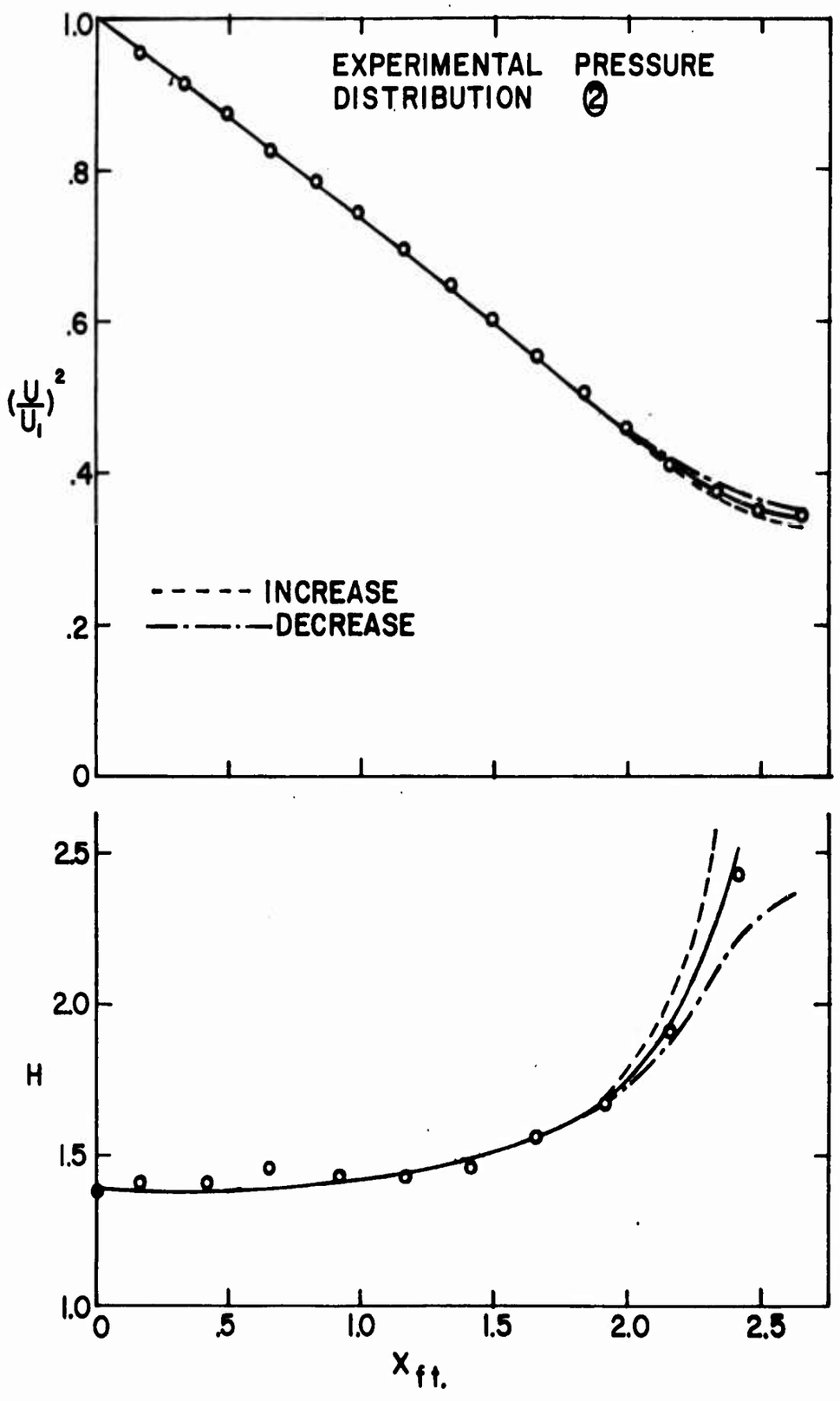

FIGURE 24. EFFECT OF ERROR IN STATIC PRESSURE

INITIAL DISTRIBUTION LIST

Copies	Organization
75	Commanding Officer and Director David Taylor Model Basin Washington 7, D. C. Attn: Code 513
7	Chief, Bureau of Ships Department of the Navy Washington 25, D. C. Attn: Technical Library Code 210 L (3) Code 420 (1) " 341 B (1) " 421 (1) " 345 (1)
1	Office of Naval Research Branch Office, Forrestal Research Center Princeton, N. J. Attn: Mr. J. Levy
	Office of Naval Research Department of the Navy Washington 25, D. C.
1	Attn: Head, Mechanics Branch
1	Attn: Head, Fluid Dynamics Branch
1	Attn: Head, Power Branch, Code 429
	Massachusetts Institute of Technology Cambridge 39, Mass.
1	Attn: Prof. A. Shapiro
1	Prof. E. S. Taylor
1	Prof. P. G. Hill
	The Johns Hopkins University Baltimore, Maryland
1	Attn: Prof. F. Clauser
1	Attn: Prof. L. S. G. Kovasznay
	Princeton University Princeton, N. J.
1	Attn: Prof. S. M. Bogdonoff
1	Prof. W. D. Hayes
1	Prof. S. I. Cheng
1	Prof. L. Crocco
1	Prof. H. Lam
1	Prof. L. Brush
1	Prof. W. O. Criminale
1	Prof. D. C. Hazen
1	Engineering Library
1	Forrestal Library

Copies	Organization
	Stanford University Department of Mechanical Engineering Stanford, California
1	Attn: Prof. S. J. Kline
1	Prof. J. P. Johnston
	University of California Berkeley, California
1	Attn: Prof. G. M. Cocos
	Harvard University Cambridge 38, Massachusetts
1	Attn: Prof. R. E. Kronauer
1	Prof. H. Emmons
	Dartmouth College Hanover, New Hampshire
1	Attn: Prof. R. C. Dean, Jr.
1	Dr. H. Eichenberger Ingersoll-Rand Co. Research and Development Bedminster, N. J.
	Westinghouse Electric Corp. Lester, Penna.
1	Attn: Mr. R. E. McNair
1	Mr. G. Howard
1	Dr. Howard Baum Department R510 AVCO Research and Advanced Development Wilmington, Mass.
1	Dr. D. C. Prince General Electric Co. Evendale, Ohio
1	Dr. D. M. Gibson General Dynamics Fort Worth, Texas
1	Dr. F. C. W. Olson U. S. Naval Mine Defense Laboratory Panama City, Florida
	Iowa Institute of Hydraulic Research University of Iowa Iowa City, Iowa
1	Attn: Dr. Hunter Rouse
1	NASA 1512 H. Street, N. W. Washington 25, D. C.

Copies	Organization
	University of Delaware Newark, Delaware
1	Attn: Prof. J. Hartnett
1	Dr. J. A. Schetz General Applied Science Lab., Inc. Westbury, L. I., New York
	University of Minnesota St. Anthony Falls Hydraulic Laboratory Minneapolis 14, Minn.
1	Attn: Director
	Aeronautical Research Associates at Princeton Princeton, N. J.
1	Attn: Dr. C. DuP. Donaldson, President
1	Dr. L. Landweber Iowa Institute of Hydraulic Research University of Iowa Iowa City, Iowa
1	Mr. Neal Tetervin Naval Ordnance Laboratory White Oak Silver Spring, Maryland
1	Dr. F. R. Hama Jet Propulsion Laboratory Pasadena, California
1	Dr. G. B. Schubauer National Hydraulic Laboratory Bureau of Standards Washington, D. C.
1	Dr. D. Coles California Institute of Technology Pasadena, California
1	Dr. J. M. Robertson University of Illinois Urbana, Illinois
1	Mr. E. M. Uram Davidson Laboratory Stevens Institute of Technology Hoboken, N. J.
1	Mr. W. B. Giles Ordnance Department General Electric Co. Pittsfield, Mass.

Copies	Organization
1	Dr. J. J. Cornish, III Department of Aerophysics Mississippi State University State College, Miss.
1	Dr. Paul Kaplan Oceanics, Inc. Technical Industrial Park Plainview, L. I. , New York
1	Prof. Irving Michelson Illinois Institute of Technology Technology Center Chicago 16, Ill.
1	Prof. D. A. Nesmith Engineering Experiment Station Kansas State University Manhattan, Kansas 66504
1	Editor, Engineering Index Engineering Societies Library 29 West 39th. Street New York 18, N. Y.
1	Editor, Applied Mechanics Reviews Southwest Research Institute 8500 Culebra Road San Antonio 6, Texas
	Office of Naval Research, Boston Branch 495 Summer Street Boston 10, Mass.
1	Attn: Commanding Officer
1	Dr. F. B. Gardner
1	Mr. T. B. Dowd
1	Commanding Officer Office of Naval Research, New York Branch 207 West 24th. Street New York 11, N. Y.
1	Commanding Officer Office of Naval Research, Chicago Branch 86 East Randolph Street Chicago 1, Ill.
1	Commanding Officer Office of Naval Research, San Francisco Branch 1000 Geary Street San Francisco 9, Calif.
1	Commanding Officer Office of Naval Reasearch, Pasadena Branch 1030 East Green Street Pasadena 1, Calif.

Copies	Organization
1	Prof. G. L. Mellor Department of Mechanical Engineering Princeton University Princeton, N. J.
1	Mr. M. P. Tulin HYDRONAUTICS, Inc. Pindell School Road, Laurel Howard County, Maryland
1	Dr. D. L. Turcotte Graduate School of Aeronautical Engineering Cornell University Ithaca, New York
1	Prof. E. A. Eichelbrenner Department of Mechanical Engineering Syracuse University Ithaca, New York
1	Mr. A. M. O. Smith Douglas Aircraft Compnay, Inc. Aircraft Division Long Beach, Calif.
1	Prof. G. H. Toebes School of Engineering Purdue University Lafayette, Indiana
	General Electric Company 570 Lexington Avenue New York 22, N. Y.
1	Attn: Mr. F. P. McCune, Vice Pres. Engineering Mr. C. H. Linder, Gen. Mgr. Turbine Div.
	Large Steam Turbine Div. General Electric Co. Schenectady 5, N. Y.
1	Attn: Mr. Carl Shabtach, Mgr. Engineering
1	Mr. J. E. Fowler
1	Mr. K. C. Cotton
1	Mr. J. Herzog
1	Mr. R. E. Brandon
	Gas Turbine Division General Electric Co. Schenectady 5, N. Y.
1	Attn: Mr. C. George, Mgr. Engineering
1	Mr. R. L. Hendrickson
1	Mr. B. D. Buckland
1	Mr. G. W. Schaper

Copies	Organization
	Large Steam Turbine-Generator Dept. General Electric Co. Schenectady 5, N. Y.
1	Attn: Mr. J. E. Downes, Mgr. Engineering
	Mr. C. W. Elston, Gen. Manager
	Flight Propulsion Division General Electric Co. Cincinnati 15, Ohio
1	Attn: Technical Information Center, Bldg. 100
1	Mr. D. Cochran, Gen. Manager
1	Mr. J. W. McBride, Devel. Plan. Group, Bldg. 300
1	Mr. R. G. Griffin
1	Dr. S. N. Suciu, Mgr. Appl. Res. Oper., Bldg. 300
	Small Aircraft Engine Division General Electric Co. 1000 Western Ave. Lynn, Mass.
1	Attn: Mr. Edward Woll, Mgr.
	Aircraft Gas Turbine Division General Electric Co. Cincinnati 15, Ohio
1	Attn: Dr. LeR. Smith, Jr.
1	Mr. E. Perugi
	Large Jet Engine Dept. General Electric Co. Evendale, Ohio
1	Attn: Mr. D. C. Berkey
	Mr. W. R. Cornell
	Mr. L. Wright
1	Mr. J. E. Knott, Director of Engineering Aircraft Engine Operations Allison Division - General Motors Corp. Indianapolis 6, Ind.
1	Mr. E. B. Newill, General Manager Allison Division - General Motors Corp. Indianapolis 6, Ind.
	Turbine Engine Dept. Allison Division - General Motors Co. Indianapolis 6, Ind.
1	Attn: Mr. J. N. Barney
1	Mr. B. A. Hopkins
1	Mr. C. R. Lowes
	Engineering Development Dept. General Motors Research Laboratories 12 Mile and Mound Roads Warren, Michigan
1	Attn: Dr. Gino Sovran
1	Mr. C. A. Amann

Copies	Organization
1	Librarian General Motors Technical Center Warren, Michigan
	National Science Foundation Washington 25, D. C.
1	Attn: Head, Engineering Section
1	Naval Liason Office Massachusetts Institute of Technology Building 20E, Room 232 Cambridge 39, Mass.
1	Library of Congress Exchange and Gift Division Washington 25, D. C.

UNCLASSIFIED